ENHANCE ENERGY CLIVE MMV PLAN

APPENDICES D:

Geomechanical Analysis of the Effects of CO_2 Injection in the Clive Leduc and Clive Nisku Reservoirs in the Clive Field

July, 2019

APPENDIX D

GEOMECHANICAL ANALYSIS OF THE EFFECTS OF CO_2 INJECTION IN THE LEDUC (D-3A) AND NISKU (D-2) RESERVOIRS IN THE CLIVE FIELD

Confidential Phase 2 Client Report to Enhance Energy Inc.

by

Alberta Innovates – Technology Futures

March 2012

Disclaimer

1. This Report was prepared as an account of work conducted at the ALBERTA INNOVATES - TECHNOLOGY FUTURES ("AITF") on behalf of Enhance Energy Inc. All reasonable efforts were made to ensure that the work conforms to accepted scientific, engineering and environmental practices, but AITF makes no other representation and gives no other warranty with respect to the reliability, accuracy, validity or fitness of the information, analysis and conclusions contained in this Report. Any and all implied or statutory warranties of merchantability or fitness for any purpose are expressly excluded. Enhance Energy Inc. acknowledges that any use or interpretation of the information, analysis or conclusions contained in this Report is at its own risk. Reference herein to any specified commercial product, process or service by trade-name, trademark, manufacturer or otherwise does not constitute or imply an endorsement or recommendation by AITF.

2. The information contained in this Report is confidential and may not be distributed, referenced or quoted without the prior written approval of Enhance Energy Inc.

3. Any authorized copy of this Report distributed to a third party shall include an acknowledgement that the Report was prepared by AITF and shall give appropriate credit to AITF and the authors of the Report.

4.

Authors

This report was prepared by a team of AITF staff comprising:

Hamidreza Soltanzadeh, Ph.D., P.Eng., Geomechanics

Alireza Jafari, Ph.D., Thermal Simulation

Tyler Hauck, M.Sc., P.Geol., Geology

Executive Summary

In Phase 1 of this project, a two dimensional mechanical earth model (MEM) was developed for the sedimentary succession overlying the Leduc (D-3A) and Nisku (D-2) reservoirs in the Clive oil field in central Alberta. This model included geomechanical characterization of the geological units from the base of the Calmar Formation, which forms the caprock of the Nisku (D-2) reservoir, to the ground surface. In the current study, this MEM was extended by adding geological units below the Calmar Formation including the Nisku, Ireton, Leduc, and Cooking Lake formations. Then, based on this complete MEM, 3D numerical modelling was conducted to study the geomechanical response of the Leduc (D-3A) and Nisku (D-2) reservoirs to historical oil and gas production and future CO_2 injection.

The numerical modeling was performed using a commercial finite-difference analysis software, FLAC3D. The geometry of the model was constructed based on the geological model developed by AITF. For the case of historical production, the average reservoir pressure variation was estimated using public domain data. For the case of CO_2 injection, the expected increase in the average reservoir pressure was estimated through communications with Enhance Energy Inc. A simplistic single-well simulation was developed to predict temperature changes induced by the injection of cooler CO_2 into these reservoirs.

To study the effects of pressure changes, a 3D geomechanical model was developed for the entire study area. The results of modeling suggested that the potential for fracturing and fault reactivation has been low during the historical producing life of the field. Therefore, it is less likely that the integrity of the caprock has been disturbed during this period. The results also showed low potential for fracturing or fault reactivation induced by future CO_2 injection. The modeling predicted a maximum surface heave of 2.4 mm as a result of the pressure build-up caused by CO_2 injection.

Sensitivity analysis confirm that the variations in the mechanical rock properties do not lead to meaningful changes in the modelling results regarding the low potential for fracturing and fault reactivation induced by pressure changes. Also, the effects of these variations on the predicted reservoir deformation and surface heave are only in order of millimetres.

To study the effects of temperature changes induced by the injection of CO_2 at temperatures lower than reservoir temperature, a single-well geomechanical model with a higher resolution was developed because of the lack of thermal interaction between injection wells. The modeling was performed based on two scenarios of 15 and 30°C for the injected CO_2 temperatures. The results of the modeling suggest that for the both cases tensile fractures are likely to occur within the reservoirs. Due to the possibility of tensile fracturing, more detailed modeling is recommended to study the geomechanical response of the surrounding rock (caprock) to temperature changes within the reservoirs. It is suggested that thermal-fluid flow simulation coupled with geomechanical

studies should be conducted. These geomechanical studies must be capable of accounting for the effects of fracture initiation and propagation on the hydraulic integrity of surrounding rock.

Alberta Innovates Technology Futures

Table of Contents

Alberta Innovates Technology Futures

List of Figures

List of Tables

1. Introduction

Enhance Energy plans to inject CO_2 in the Leduc (D-3A) and Nisku (D-2) reservoirs in the Clive Field in Alberta for enhanced oil recovery (CO_2-EOR). Furthermore, it is also planned to use these reservoirs for CO_2 storage at the end of the reservoirs' producing life. The operations of injection and production of different fluids results in pressure and temperature changes within the reservoirs and their surrounding rock. These changes usually lead to ground deformation and perturbation of *in-situ* stresses. Geomechanical analyses are required to evaluate the effect of pressure and temperature changes on the geomechanical and hydraulic integrity of the reservoirs and surrounding caprock.

In Phase 1 of this project conducted by the University of Saskatchewan (Oar et al., 2011) a Mechanical Earth Model (MEM) was developed. This model includes mechanical properties and *in-situ* stresses within the sedimentary succession from the base of the Calmar Formation, which overlies the Nisku (D-2) reservoir, to the ground surface. To perform geomechanical analyses it was necessary to complete this MEM by adding Devonian stratigraphic units in the study area including the reservoirs and the unit immediately underlying them.

The objectives of the work presented in this report were:

1. To complete the previously developed MEM by including the sedimentary succession covering the Cooking Lake, Leduc, Ireton and Nisku formations; and
2. To study the geomechanical response of the Leduc (D-3A) and Nisku (D-2) reservoirs in the Clive oil field to oil and gas production and CO_2 injection using a numerical model based on the full MEM.

2. Mechanical Earth Model (MEM)

In the first part of this chapter, a short summary of the procedure for data collection and analysis followed in Phase 1 is presented. A very similar approach was taken in the current phase to estimate the geomechanical properties of the stratigraphic units of interest below the Calmar Formation. The combined results from these two phases were upscaled to construct a MEM to be used in geomechanical modelling.

2.1 Review of Data Collection and Analysis in Phase 1

In Phase 1 of this project the geomechanical properties of the sedimentary succession above the Nisku Formation were characterized by the University of Saskatchewan (Oar et al., 2011). The characterization was performed based on the well log data from 16 wells in the study area. These results were used to construct a 2-D mechanical earth model (MEM) for the project. The developed MEM includes rock mechanical properties and *in-situ* stresses for the stratigraphic units. All the log analyses and calculations in this phase of the project were performed in Petrel (Schlumberger, 2009). A review of the characterization procedure and results is presented below.

Due to the lack of diploe shear (DSI) logs in the study area, DSI logs from other fields in the region (i.e, the Redwater, Willingdon, and Caroline fields) were used to determine dynamic Poisson's ratios (v_d) of the stratigraphic units. Compressive wave transient times (Δt_c) and densities (ρ_b) were determined from sonic and density logs, respectively. These logs were used in the following equation to calculate dynamic Young's modulus (E_d) logs.

$$E_d = \frac{\rho_b}{\Delta t_c^{\,2}} \frac{(1-2\nu_d)(1+\nu_d)}{(1-\nu_d)} \qquad (2.1)$$

where:

v_d = dynamic Poisson's ratio

E_d = dynamic Young's modulus

Δt_s = shear wave interval transit time (reciprocal of shear wave velocity)

Δt_c = compressional wave interval transit time (reciprocal of compressional wave velocity)

ρ_b = bulk density

The static values for Poisson's ratio (v_s) were assumed equal to the log-derived dynamic values and static Young's moduli (E_s) were estimated using a linear regression (i.e., E_s=0.75E_d) based on literature review. As a conservative assumption, a zero value for tensile strength was recommended. Empirical relationships (Chang et al., 2006) were used to estimate rock strength properties (i.e., friction angle (ϕ) and unconfined compressive strength (*UCS*) for each

stratigraphic unit. Using a linear Mohr-Coulomb failure criterion, cohesion (c) values were calculated from *UCS* and friction angle (ϕ) as follows:

$$c = \frac{UCS\left(1-\sin\phi\right)}{2\cos\phi} \tag{2.2}$$

Formation pore pressures (P_{fm}) in the aquifers were determined based on the data provided by AITF and pore pressures for other units were estimated from using the pressures in the adjacent aquifers. Vertical *in-situ* stresses (S_v) were calculated using density logs and a poroelastic uniaxial deformation approach (Warpinksi, 1989) was used for preliminary estimation of maximum and minimum horizontal *in-situ* stresses (i.e., respectively, S_{Hmax} and S_{hmin}) in the field according to:

$$S_{h\min} = \frac{\nu_s}{1-\nu_s}\left(S_V - \alpha p_{fm}\right) + \alpha p_{fm} + \frac{\nu_s E_s \varepsilon_{H\max}}{1-\nu_s^{\,2}} \tag{2.3}$$

$$S_{H\max} = \frac{\nu_s}{1-\nu_s}\left(S_V - \alpha p_{fm}\right) + \alpha p_{fm} + \frac{E_s \varepsilon_{H\max}}{1-\nu_s^{\,2}} \tag{2.4}$$

where ε_{Hmax} is the tectonic strain parallel to the maximum horizontal stress azimuth and its value for this study interpreted to be 6×10^{-4} from a mini-frac test located close to the study area as reported by Woodland and Bell (1989). Biot's coefficient (α) was assumed to be 1 for the rocks in this study. Previous work has shown that stress regime in the Alberta basin is of the strike-slip fault type, the maximum and minimum *in-situ* stresses in the Alberta basin are the maximum and minimum *in-situ* horizontal stresses, respectively, with the vertical stress having values between these two (Bell et al., 1994). Bachu et al. (2005) have shown that the gradient of minimum horizontal stress S_{hmin} in the Alberta basin has an average value of 16.7 kPa/m. Gradients of the vertical stress calculated for the study area reach up to 23.9 kPa/m (see Section 2.2 below). Thus, because $S_{Hmax}>S_v>S_{hmin}$, to filter unrealistic results, the calculated *in-situ* stresses from these equations were limited by a lower bound of 16 kPa/m for minimum horizontal *in-situ* stress gradient and an upper bound of 33.0 kPa/m for maximum horizontal *in-situ* stress gradient. Finally, frictional equilibrium analyses were performed to ensure that the calculated *in-situ* stresses do not exceed the frictional strength of the potentially-existing faults in the study area.

2.2 Completion of Data for the Lower Stratigraphic Units

The developed MEM in Phase 1 was completed by extending the model to include the stratigraphic units of interest below the Calmar Formation, i.e., the Nisku, Ireton, Leduc, and Cooking Lake formations. A similar approach to Phase 1 was followed to characterize the mechanical properties of these formations.

Sixteen wells in the study area and in its close vicinity were selected for this study (Figure 1). The criterion for selecting these wells was availability of the required well logs for

geomechanical characterization of the desired stratigraphic units. All the log data for these wells were acquired from geoSCOUT database (geoLOGIC Systems Ltd., 2011) and log analyses were performed using the Prizm module of GeoGraphix Discovery Suite (LMKR, 2011). An example of the results of the calculations of Young's modulus and *in-situ* stresses for a representative well (100/09-03-039-24W4/00) is shown in Figure 2. Appendix A includes the methodology and details of strength properties calculation for each stratigraphic unit.

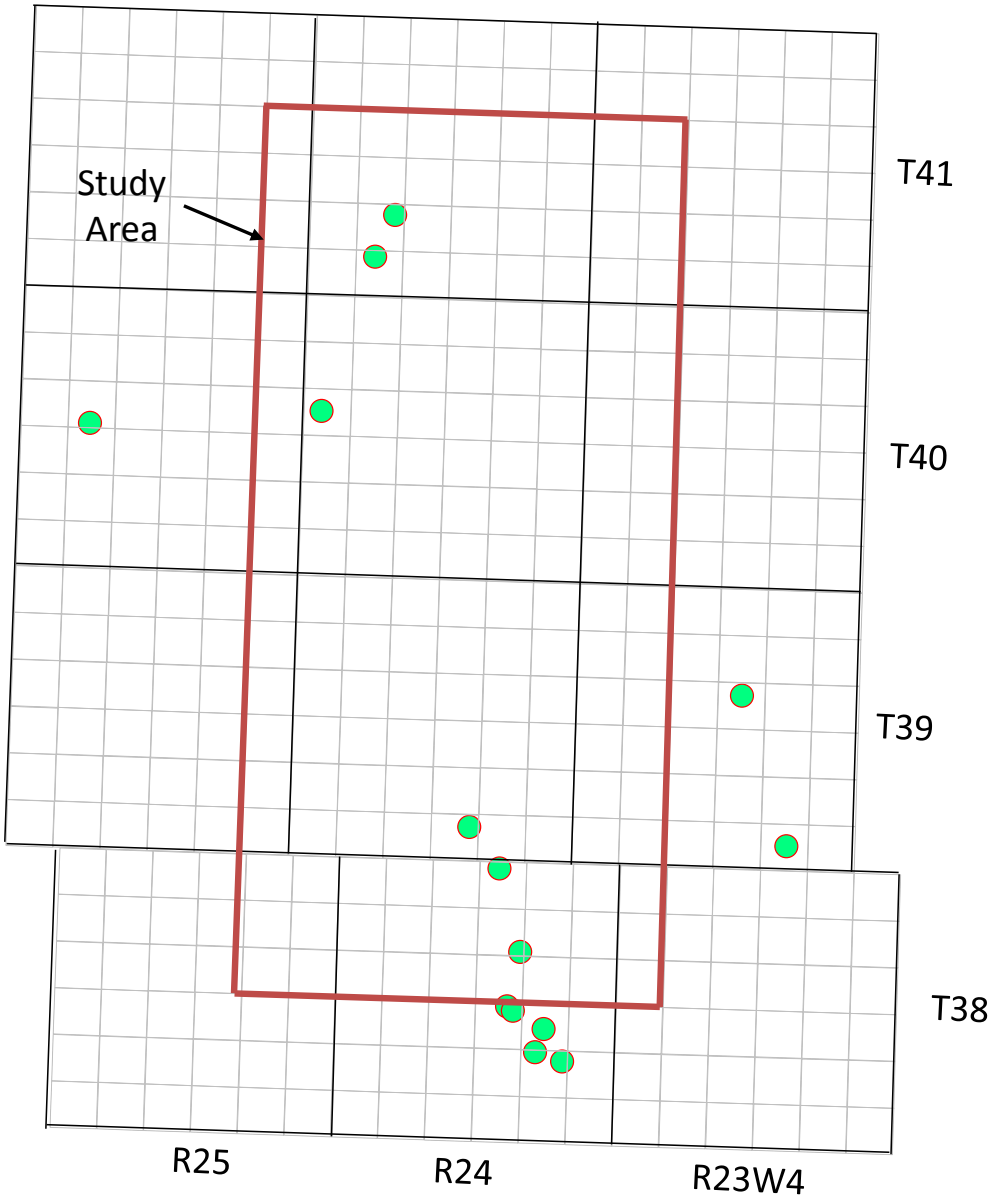

Figure 1: Location of wells with logs used for calculation of rock mechanical properties in Phase 2 of the project.

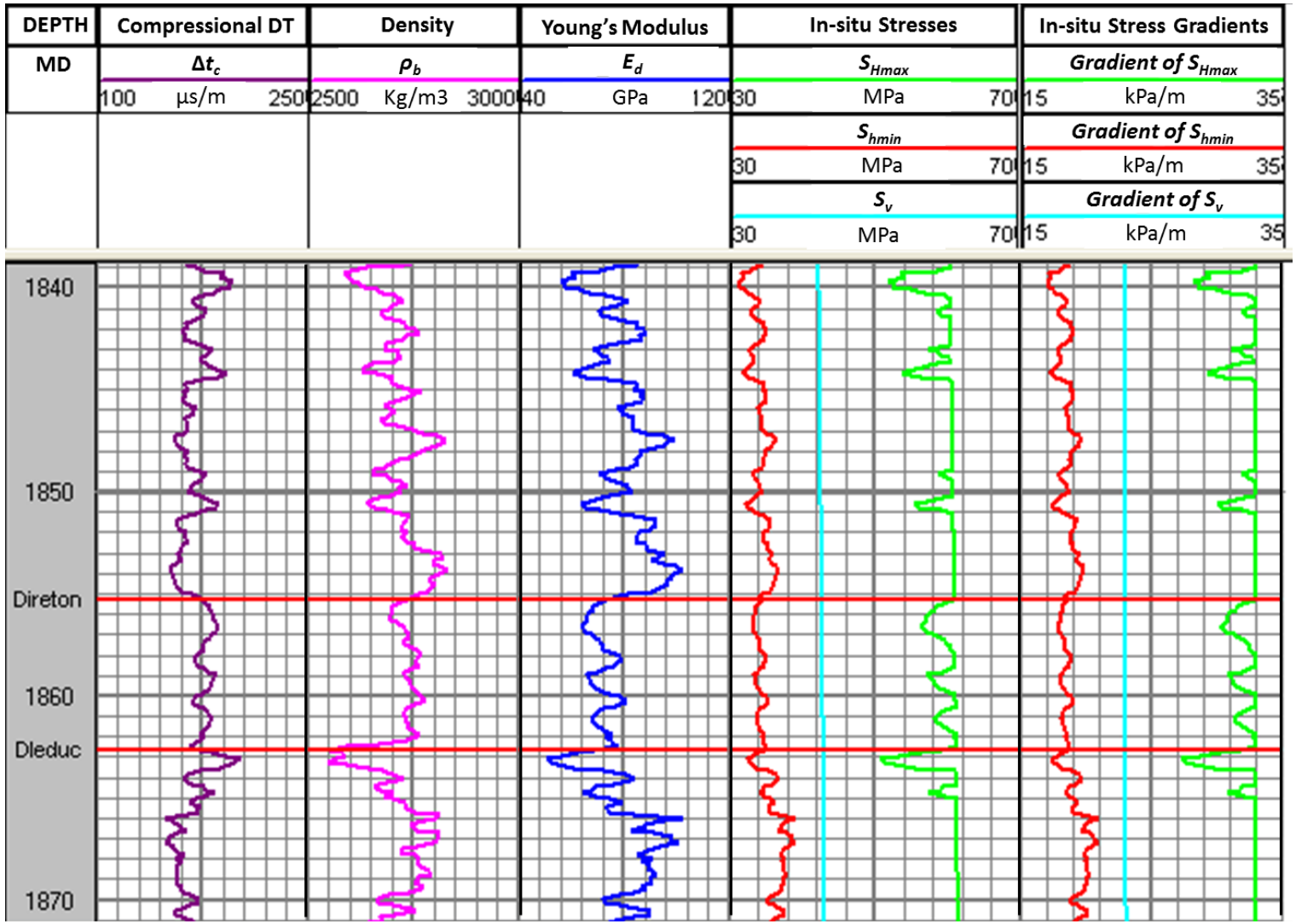

Figure 2: Performed log analyses to determine geomechanical properties for the Leduc, Ireton and Nisku formations in well 100/09-03-039-24W4/00 using PRISM (LMKR, 2011)

2.3 Property Upscaling

In the first level of upscaling (i.e., well upscaling), for each property profile in each well, an average value was taken for each stratigraphic unit to use as a representative value. Each of these values was assumed to represent the magnitude of each property for each stratigraphic unit in the immediate vicinity of each well. For all parameters except Young's modulus, an arithmetic average was calculated. For Young's modulus, the use of a geometric average was considered more appropriate (Oar et al., 2011). The detailed results of these calculations and their statistical interpretations are given in Appendix B of this report.

In the second level of upscaling (i.e., formation upscaling), the property values at each of the well location for each stratigraphic units has been statistically analysed to determine the minimum, maximum, mean, and standard deviation for each property. The results of these analyses are shown in Tables 1 and 2, respectively. Based on these tables, the maximum relative standard deviation (~18%) for Young's modulus occurs for the Exshaw Formation, with an average of 21.6 GPa and a standard deviation of 3.8 GPa. The values of relative standard deviation for Young's modulus are considerably lower for many stratigraphic units in the study area. The maximum value of relative standard deviation for *in-situ* stresses is less than 6%.

It was anticipated that such variations in mechanical properties would have a negligible impact on the results of geomechanical analyses; this has been confirmed by running a number of sensitivity analyses as will be seen later in this report. Therefore, it was decided to assign the single-value average for each property to each stratigraphic unit in the entire study area. Table 3 summarizes the calculated averaged values of each property for each stratigraphic unit. Upscaling to a 3-D MEM was undertaken by assigning the averaged values presented in Table 2 to the corresponding stratigraphic units in the geological model.

Alberta Innovates Technology Futures

Table 1: Statistical summary of the MEM properties for the stratigraphic succession above the base of Calmar Formation (Oar et al., 2011)

Strat. Unit	Static Poisson's Ratio	Static Young's Modules, E_s (GPa)				Vertical Stress (S_v) Gradient (kPa/m)				Min. Horizontal Stress (S_{hmin}) Gradient (kPa/m)				Max. Horizontal Stress (S_{Hmax}) Gradient (kPa/m)				*UCS* (MPa)	ϕ (°)
	Mean	Min	Max	Mean	Std. Dev.	Min	Max	Mean	Std. Dev.	Min	Max	Mean	Std. Dev.	Min	Max	Mean	Std. Dev.	Mean	Mean
Above Upper Belly River	**0.39**	5.9	8.0	**6.8**	0.5	18.9	23.0	**21.4**	1.2	18.4	21.4	**20.3**	0.9	22.5	26.7	**25.3**	1.2	**10**	**40**
Upper Belly River	**0.39**	8.0	9.5	**8.6**	0.4	19.5	22.9	**21.5**	0.8	16.4	19.8	**18.2**	0.9	20.4	24.9	**23.1**	1.2	**14**	**40**
Basal Belly River	**0.39**	9.3	13.4	**11.0**	1.1	20.1	23.0	**21.7**	0.7	18.1	20.7	**19.2**	0.7	22.7	26.6	**24.3**	1.1	**23**	**40**
Lea Park	**0.41**	7.4	8.9	**8.1**	0.4	20.2	23.1	**21.8**	0.7	18.7	21.4	**20.0**	0.7	22.7	26.6	**24.5**	1.0	**14**	**32**
Milk River	**0.40**	7.7	9.7	**8.7**	0.6	20.3	23.1	**21.7**	0.7	18.2	20.2	**19.2**	0.6	22.1	24.4	**23.3**	0.7	**16**	**32**
Colorado	**0.38**	10.3	12.2	**11.4**	0.5	20.8	23.2	**21.9**	0.7	17.4	18.9	**18.3**	0.5	21.5	23.6	**22.5**	0.7	**17**	**33**
2nd White Speck	**0.36**	10.2	12.0	**11.4**	0.5	21.2	23.4	**22.2**	0.6	16.4	17.6	**17.1**	0.4	20.0	21.6	**20.9**	0.5	**46**	**41**
Viking	**0.36**	10.3	12.8	**11.7**	0.6	21.3	23.4	**22.2**	0.6	16.6	18.2	**17.4**	0.4	20.6	23.1	**21.6**	0.6	**19**	**40**
Viking Sandstone	**0.36**	15.5	17.3	**16.2**	0.5	21.3	23.5	**22.3**	0.6	16.2	18.0	**17.0**	0.5	19.3	22.5	**20.7**	0.8	**32**	**40**
Joli Fou	**0.40**	5.0	7.4	**6.5**	0.7	21.3	23.5	**22.3**	0.6	17.4	19.9	**18.8**	0.7	19.4	23.9	**21.9**	1.4	**10**	**29**
Mannville	**0.32**	19.0	22.1	**20.7**	0.9	21.4	23.5	**22.3**	0.6	16.0	17.4	**16.4**	0.4	19.5	24.6	**21.1**	1.3	**13**	**40**
Glauconitic	**0.31**	18.9	29.1	**22.0**	2.5	21.5	23.5	**22.4**	0.6	16.2	18.4	**17.3**	0.5	21.8	26.7	**24.4**	1.3	**38**	**40**
Ostracod	**0.29**	21.4	27.5	**24.2**	1.5	21.6	23.6	**22.4**	0.6	16.2	17.4	**16.7**	0.4	22.5	26.3	**24.5**	1.1	**28**	**37**
Ellerslie	**0.29**	23.7	27.4	**25.7**	1.0	21.6	23.6	**22.5**	0.6	16.0	18.0	**17.0**	0.6	21.7	28.6	**25.1**	2.2	**43**	**40**
Banff	**0.29**	19.1	20.8	**20.1**	0.9	22.0	22.5	**22.2**	0.3	16.0	16.1	**16.0**	0.1	20.8	22.4	**21.6**	0.8	**20**	**35**
Exshaw	**0.29**	16.8	27.6	**21.6**	3.8	22.0	23.6	**22.5**	0.6	16.1	17.0	**16.7**	0.4	22.0	25.6	**23.9**	1.1	**22**	**36**
Wabamun	**0.27**	34.3	58.3	**50.1**	5.2	21.7	23.7	**22.6**	0.5	16.9	18.6	**17.8**	0.5	27.2	32.0	**29.4**	1.4	**138**	**32**
Stettler	**0.24**	63.5	68.4	**65.5**	1.7	22.0	23.4	**22.8**	0.5	16.7	18.9	**17.7**	0.6	28.8	33.0	**31.8**	1.4	**138**	**32**
Calmar	**0.24**	46.1	57.7	**52.6**	3.9	22.2	23.7	**23.0**	0.5	17.6	19.0	**18.5**	0.5	30.6	33.0	**32.4**	0.8	**65**	**43**

Alberta Innovates Technology Futures

Table 2: Statistical summary of the MEM properties for the stratigraphic succession of interest below the Calmar Formation

Strat. Unit	Static Poisson's Ratio	Static Young's Modules, E_s (GPa)				Vertical Stress (S_v) Gradient (kPa/m)				Min. Horizontal Stress (S_{hmin}) Gradient (kPa/m)				Max. Horizontal Stress (S_{Hmax}) Gradient (kPa/m)				*UCS* (MPa)	ϕ (°)
	Mean	Min	Max	Mean	Std. Dev.	Min	Max	Mean	Std. Dev.	Min	Max	Mean	Std. Dev.	Min	Max	Mean	Std. Dev.	Mean	Mean
Nisku	**0.24**	61.0	77.3	**69.5**	4.4	22.9	23.9	**23.4**	0.3	16.0	19.9	**19.1**	0.9	32.1	33.0	**32.8**	0.3	**199**	**40**
Ireton	**0.25**	49.5	67.8	**59.2**	5.5	22.9	23.9	**23.4**	0.3	16.0	19.8	**18.8**	1.0	30.1	33.0	**32.1**	1.0	**78**	**45**
Leduc	**0.26**	45.1	66.5	**57.4**	7.3	23.0	23.9	**23.4**	0.3	16.0	20.1	**19.0**	1.1	28.3	33.0	**31.8**	1.4	**160**	**40**
Cooking Lake	**0.26**	45.1	66.5	**57.4**	7.3	23.0	23.9	**23.4**	0.3	16.0	20.1	**19.0**	1.1	28.3	33.0	**31.8**	1.4	**160**	**40**

Alberta Innovates Technology Futures

Table 2: Upscaled property values for different stratigraphic units in the Clive MEM

Stratigraphic Unit	Static Poisson's ratio	Static Young's Moduls, E_s (GPa)	Vertical Stress (S_v) Gradient (kPa/m)	Minimum Horizontal Stress (S_{hmin}) Gradient (kPa/m)	Maximum Horizontal Stress (S_{Hmax}) Gradient (kPa/m)	*UCS* (MPa)	Friction Angle, ϕ (°)
Above Upper Belly River	0.39	6.8	21.4	20.3	25.3	10	40
Upper Belly River	0.39	8.6	21.5	18.2	23.1	14	40
Basal Belly River	0.39	11.0	21.7	19.2	24.3	23	40
Lea Park	0.41	8.1	21.8	20.0	24.5	14	32
Milk River	0.40	8.7	21.7	19.2	23.3	16	32
Colorado	0.38	11.4	21.9	18.3	22.5	17	33
2nd White Speck	0.36	11.4	22.2	17.1	20.9	46	41
Viking	0.36	11.7	22.2	17.4	21.6	19	40
Viking Sandstone	0.36	16.2	22.3	17.0	20.7	32	40
Joli Fou	0.40	6.5	22.3	18.8	21.9	10	29
Mannville	0.32	20.7	22.3	16.4	21.1	13	40
Glauconitic	0.31	22.0	22.4	17.3	24.4	38	40
Ostracod	0.29	24.2	22.4	16.7	24.5	28	37
Ellerslie	0.29	25.7	22.5	17.0	25.1	43	40
Banff	0.29	20.1	22.2	16.0	21.6	20	35
Exshaw	0.29	21.6	22.5	16.7	23.9	22	36
Wabamun	0.27	50.1	22.6	17.8	29.4	138	32
Stettler	0.24	65.5	22.8	17.7	31.8	138	32
Calmar	0.24	52.6	23.0	18.5	32.4	65	43
Nisku	0.24	69.5	23.4	19.1	32.8	199	40
Ireton	0.25	59.2	23.4	18.8	32.1	78	45
Leduc	0.26	57.4	23.4	19.0	31.8	160	40
Cooking Lake	0.26	57.4	23.4	19.0	31.8	160	40

3. Data Collection and Processing for Geomechanical Analysis

The data required for a geomechanical model of a reservoir and the rocks surrounding it may be categorized into three main groups: i) geological structure (i.e., model geometry); ii) rock mechanical properties; iii) pore pressure; and iv) temperature. The following sections describe the process of data collection for each data group for the geomechanical models developed in this project.

3.1 Geological Structure

The geological structure of this model is based on the initial geological model developed for the project by AITF. The developed geological model in Phase 1 of this project (AITF, 2011) only included the sedimentary succession from the base of the Calmar Formation (top of Nisku Formation) to the ground surface. In this phase of the project, the geological model was extended to include the lower stratigraphic units including the Nisku, Ireton, Leduc, and Cooking Lake formations. The geographical limits of the project study area are limited to townships 38 to 45 and ranges 23 -25 west of the fourth meridian (Figure 1). The geological model comprises 26 horizons (surfaces) and 25 associated isopachs.

The target zones for CO_2 injection are the Nisku (D-2) and Leduc (D-3A) reservoirs. The peripheral boundaries of the reservoirs and their water/oil contact elevations were provided by Enhance Energy Inc. Figure 3 shows the three-dimensional representation of the Leduc and Nisku units, their constituent reservoirs, and their immediate caprocks (i.e., the Ireton and Calmar formations, respectively,) as developed in FLAC3D (Itasca Consulting Group, 2009). For reasons discussed in the following section, the geometry used for geomechanical modeling was simplified by lumping together some of the geological stratigraphic units. More specifically, the geological model and 3D MEM were used to produce a geomechanical model containing a total of 12 mechanical stratigraphic units (Figure 4).

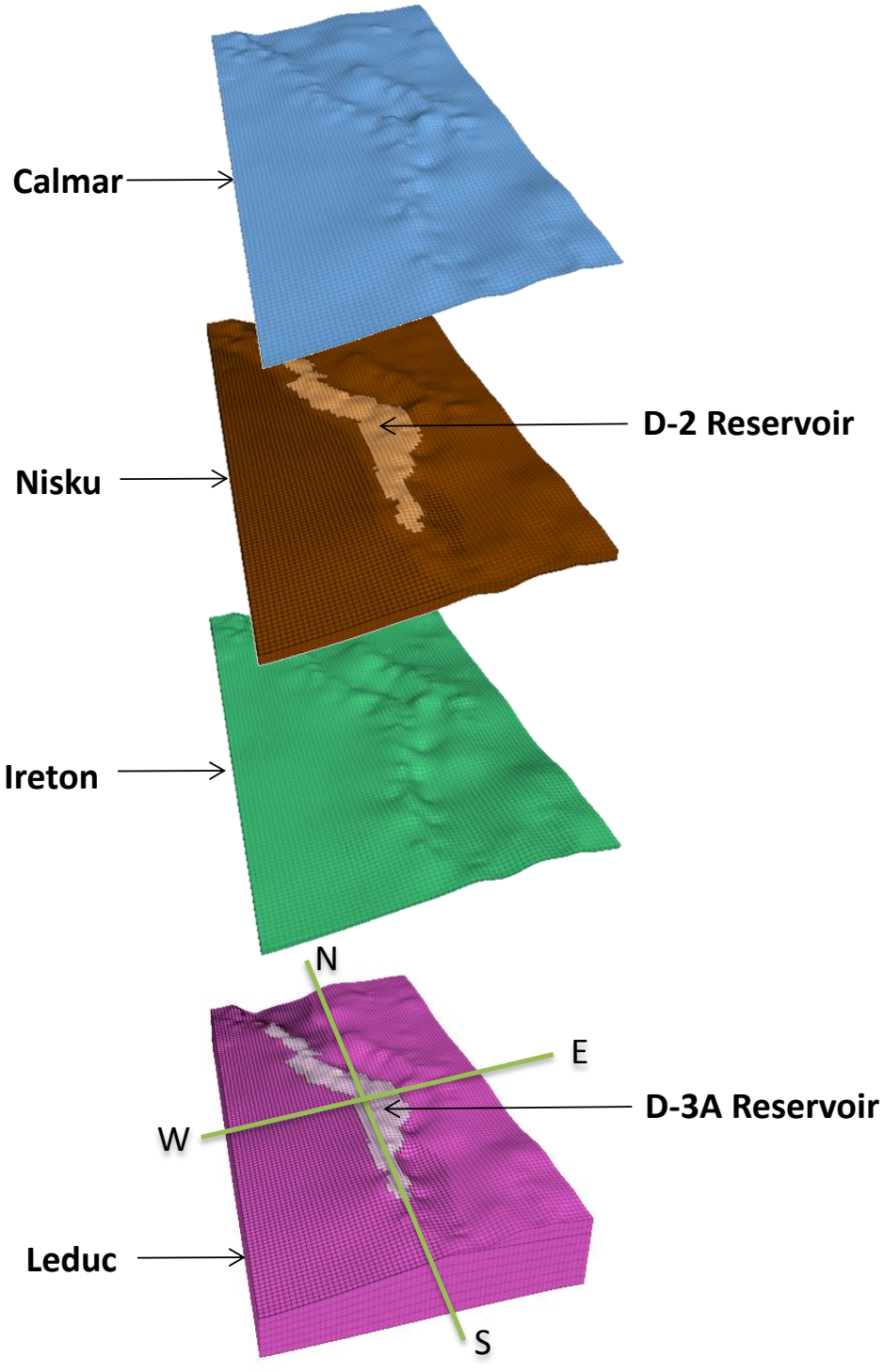

Figure 3: Exploded view of the Nisku and Leduc units, their constituent reservoirs, and their immediate caprocks. The vertical scale has been exaggerated.

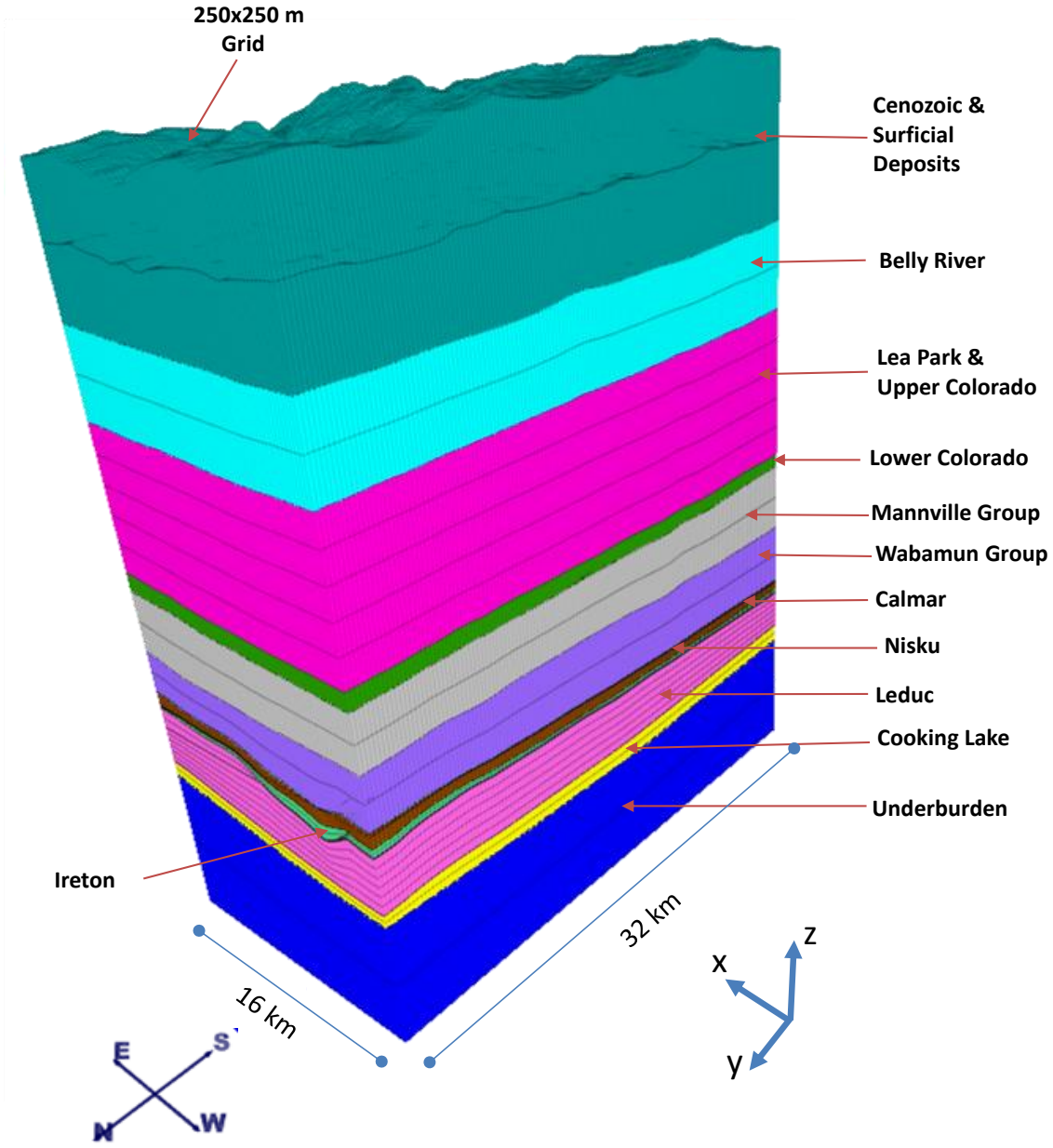

Figure 4: Three-dimensional perspective view of the mechanical stratigraphic units used in the 3D geomechanical model developed for the Clive Project using FLAC3D (Itasca Consulting Group, 2009). The vertical scale has been exaggerated.

3.2 Rock Mechanical Properties

The main source for mechanical properties is the developed MEM as described in Chapter 2 of this report. This model includes Poisson's ratio, Young's modulus, *in-situ* stresses and rock strength properties (i.e., cohesion and friction angle) for each stratigraphic unit (Table 3).

Because some of the mechanical stratigraphic units in MEM do not exist in the geological model and for practical reasons (i.e., limitations on model development time and computation time), and due to the limited sensitivity of the model to the properties of the overburden (e.g., Soltanzadeh and Hawkes, 2011), some stratigraphic units have been lumped together to define a coarser mechanical stratigraphy in the overburden (i.e., in the sequence overlying the caprock of the Nisku Formation). Material properties for these mechanical stratigraphic units have been calculated by weighted averaging by interval thickness of the mechanical properties of their constituent stratigraphic units. The mechanical properties for the entire underburden have been assumed to be same as for the Cooking Lake Formation.

Table 4 presents the thickness-weighted average properties calculated for each mechanical unit in the model. Arithmetic weighted averaging has been used for all of the properties except Young's modulus, for which Soltanzadeh and Hawkes (2011) argued that a geometrical averaging procedure is more appropriate. As an example of mechanical properties in the developed 3D geomechanical model, Figure 5 shows the variation of Young's modulus throughout the model domain.

As recommended in the Phase 1 of this project (Oar et al., 2011), the maximum horizontal *in-situ* stress was estimated to be oriented 55 degrees clockwise from north. A linear expansion coefficient (λ) of 1×10^{-5} /°C was considered for the reservoir rocks in this model (Encyclopedia Britannica, 2012).

Alberta Innovates Technology Futures

Table 3: Property values for mechanical stratigraphic units in the HARP geomechanical model

Mechanical Unit	Description	Average Thickness (m)	Static Poisson's Ratio	E_s (GPa)	S_v Gradient (MPa)	S_{hmin} Gradient (MPa)	S_{Hmax} Gradient (MPa)	*UCS* (MPa)	Friction Angle, ϕ (Degrees)	Cohesion *c* (MPa)
Cenozoic and Surficial Deposits	Surficial units above the Belly River formation	513	0.39	6.8	21.4	20.3	25.3	10	40	2.3
Belly River	Belly River and Belly River Sandstone units	306	0.39	8.7	21.5	18.2	23.1	14	40	3.3
Lea Park & Colorado	Lea Park and upper Colorado shale units	539	0.39	9.8	21.9	18.7	22.8	23	35	5.9
Lower Colorado	Lower Colorado units from the top of Viking	62	0.37	10.8	22.3	17.6	21.2	23	37	5.5
Mannville Group	Mannville Group	227	0.31	22.3	22.4	16.7	23.0	26	39	6.1
Wabamun Group	Wabamun Group	181	0.24	63.9	22.8	17.7	31.6	138	32	38.3
Calmar	Calmar formation	3	0.24	52.6	23.0	18.5	32.4	65	43	14.1
Nisku	Nisku formation	40	0.24	69.5	23.4	19.1	32.8	199	40	46.4
Ireton	Ireton formation	13	0.25	59.2	23.4	18.8	32.1	78	45	16.2
Leduc	Leduc formation	235	0.26	57.4	23.4	19.0	31.8	160	40	37.3
Cooking Lake	Cooking Lake formation	?	0.26	57.4	23.4	19.0	31.8	160	40	37.3
Underburden	Below Cooking Lake	541	0.26	57.4	23.4	19.0	31.8	160	40	37.3

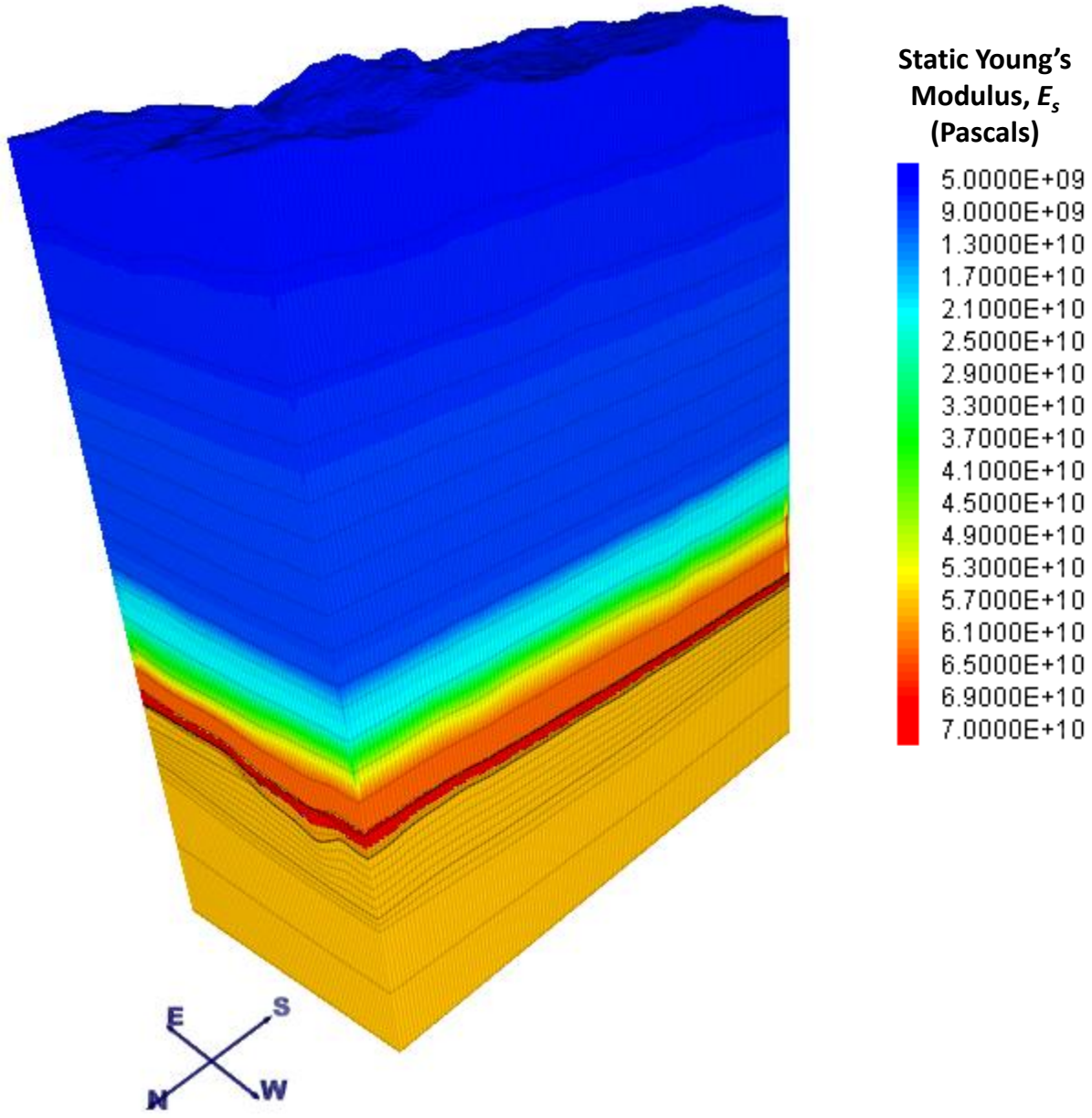

Figure 5: Distribution of Young's Modulus (in Pascals) interpreted for the 3D geomechanical model. The vertical scale has been exaggerated.

3.3 Pore Pressure Changes

The Clive oil and gas field has a long history of production and water flooding since 1952. The field includes the Nisku (D-2) the Leduc (D-3A) reservoirs with the Ireton Formation located between them. It has been indicated that, due to the breach of the Ireton Formation at several locations, the two reservoirs are hydraulically connected (Hearn et al., 2011). The historical pressure data during the life time of the reservoirs are shown in Figure 6. This figure demonstrates that an average initial reservoir pressure of about 2400 psi (16.5 MPa) had been reduced to an average of almost 1800 psi (12.5 MPa) in 2006. It was assumed that at the start of CO_2 injection the pressure will be around this value.

In absence of fluid flow simulations for CO_2 injection, as agreed with the Enhance Energy Inc., it was assumed that the reservoir pressure will uniformly increase by an average of 300 psi (2 MPa) as a result of CO_2 injection.

For the purpose of geomechanical modeling, uniform distributions of these average pressures were assumed within the regions of pressure variation. These regions were assumed to be: i) laterally confined to the reservoirs' peripheral boundaries and ii) vertically limited to the entire Nisku and Leduc formations.

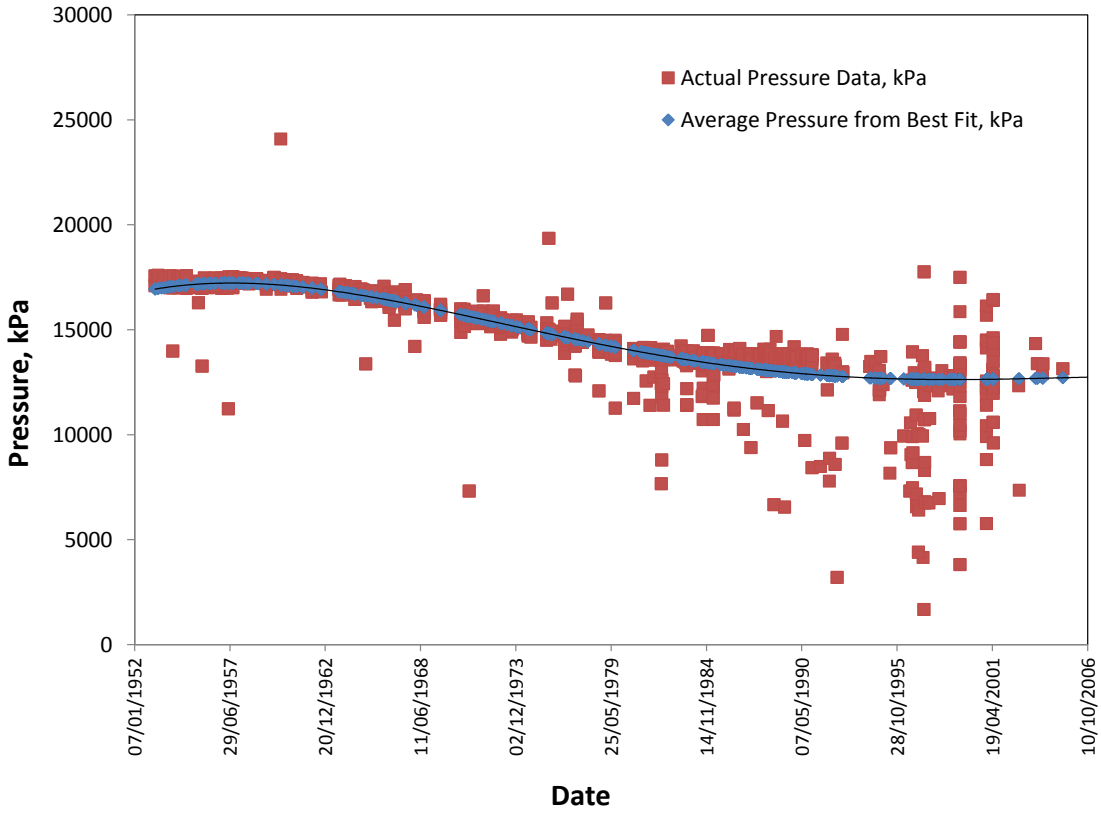

Figure 6: Pressure history of the Nisku (D-2) and Leduc reservoirs (D-3A) in the Clive oil field.

3.4 Temperature Changes

In absence of any thermal simulation to assess the effects of CO_2 injection within the reservoirs, a simplistic homogeneous single-well radial numerical model was developed by AITF for the Nisku (D-2) and Leduc (D-3A) reservoirs. A detailed description of this model is given in Appendix C. A representative initial temperature of 65°C for the reservoirs was assigned to the entire model. Figure 7 shows the temperature profiles predicted by this model after 30 years of CO_2 injection with an injection rate of 100,000 m^3/day. These results were generated for both scenarios of injected CO_2 temperatures of 15°C and 30°C. This figure indicates that in both scenarios the zone thermally influenced by CO_2 injection (i.e., the zone of temperature disturbance) is limited to an area with a radius of approximately 200 m around the injection well. This is much less than the distance between the wells considered for CO_2 injection in the field (Figure 8). Therefore, it was concluded that the assumption of a single-well model for thermal and geomechanical modeling is reasonable.

As will be shown later in this report, the results generated by these simulations have been used to assess the geomechanical response of the model to the thermal effects of CO_2 injection. However, it must be emphasized that this simplistic model does not capture many of specific characters of the field and may not be an accurate representation of the thermal field and more detailed and realistic models are required to ensure the reliability of the results.

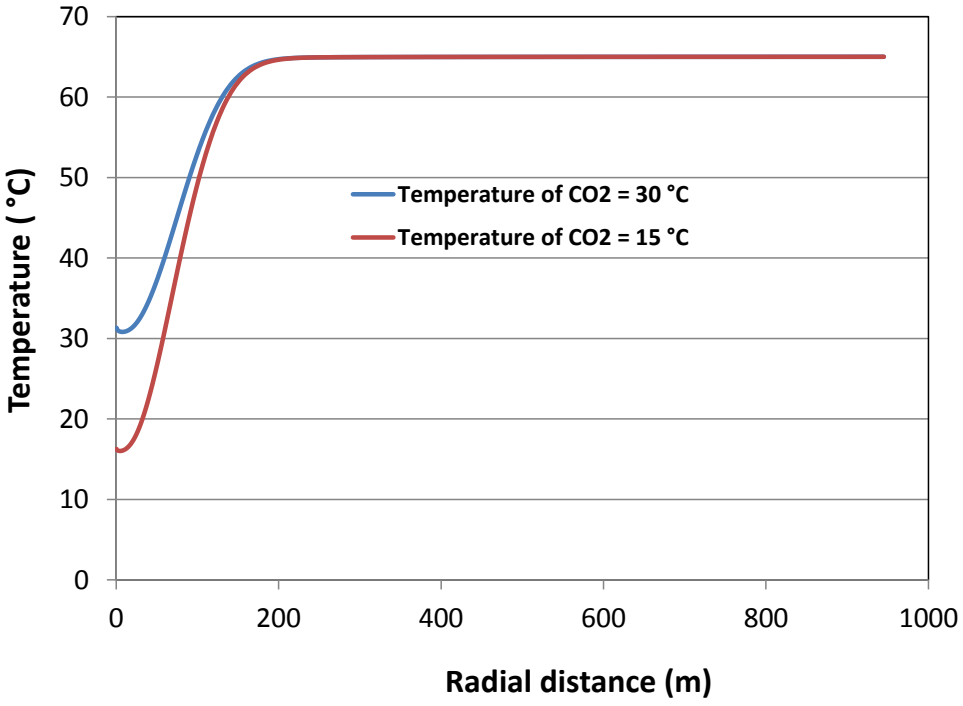

Figure 7: Profile of temperature change for two scenarios of injected CO_2 temperatures of 15°C and 30°C. A simplistic homogeneous single-well model was used to generate these results.

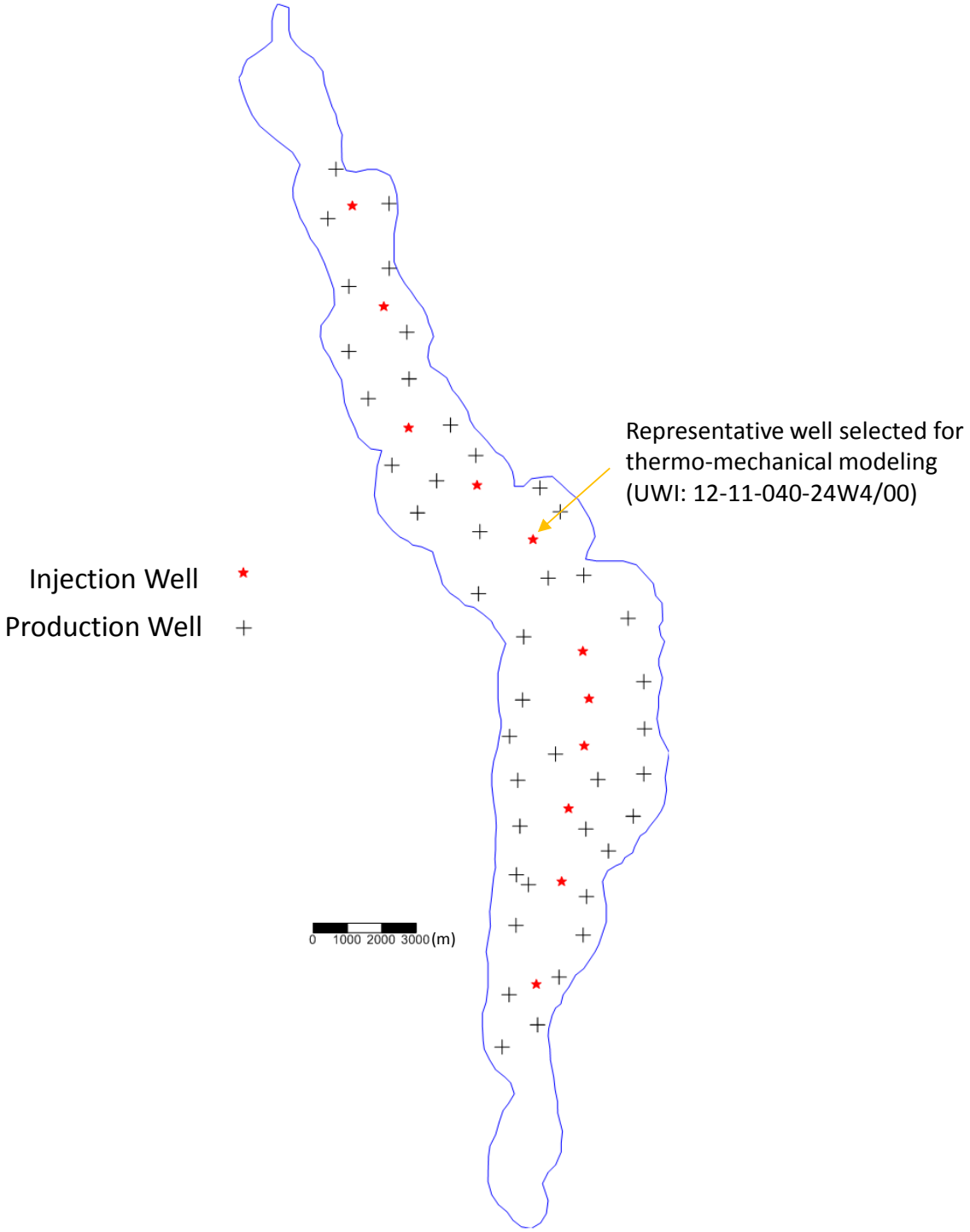

Figure 8: Plan view of the locations of planned CO_2 injection and production wells for the Nisku (D-2) reservoir in the Clive field. Data provided by Enhance Energy Inc.

4. Geomechanical Modeling

4.1 Model Characteristics

The 3D geomechanical modeling presented in this report was performed using FLAC3D (Itasca Consulting Group, 2009). This software uses the finite difference method to solve the stationary form of the linear elastic equilibrium field equations for a solid material. A total of 335,872 brick (i.e., octahedron) solid zones were used in this model. A zero-displacement boundary condition was set for the bottom surface of the model domain (elevation of -1800 m, more than 500 m below the Cooking Lake Formation), while the lateral boundaries were fixed in the horizontal direction and free in the vertical direction, and the top surface (i.e., ground surface) was a free surface. Sensitivity analyses were performed to ensure that boundary effects on modeling results are negligible.

The Coulomb criterion was used as a criterion for rock failure in this work. In this report the Strength-Stress Ratio for Fracturing ($SSR_{fracturing}$) was used to quantify the potential for intact rock failure as a result of pore pressure and/or temperature change. A value of 1.0 or less for *SSR* means that, based on the Coulomb failure criterion, failure of intact rock is predicted. Higher values mean that the rock is still behaving elastically.

Assuming a conservative value of zero for fault cohesion, the Coulomb failure criterion was also used to quantify the potential for fault reactivation. The fault friction angle was assumed to be 30 degrees in this work. The Strength-Stress Ratio for Fault Reactivation ($SSR_{reactivation}$) was used to quantify the potential for fault reactivation. A value of 1.0 or less for $SSR_{reactivation}$ means that fault reactivation is likely for critically-oriented faults. Higher values indicate no likelihood for fault reactivation. This approach for quantification of fault reactivation is conservative, since it has been developed for faults that are critically oriented with respect to the *in-situ* stress regime. Such faults, whose existence has not been proven, would be most prone to reactivation.

4.2 Geomechanical Analysis of Pore Pressure Changes

As explained in Section 3.3, this analysis assumed that the pore pressure within the reservoirs uniformly decreased by 4 MPa (600 psi) during the production history of the field. It was also assumed that pressure in the reservoirs is expected to uniformly increase by 2 MPa (300 psi) as a result of CO_2 injection. Figures 9 through 11 show the distributions of predicted induced stress changes in the model domain after oil production and CO_2 injection. These distributions were calculated by 3D geomechanical analysis, and are presented for the two cross-sections shown in Figure 3; one being oriented north-south and the other east-west.

Figure 12 shows the distribution of strength-stress ratio for fracturing ($SSR_{fracturing}$) and fault reactivation ($SSR_{reactivation}$) for the north-south and east-west cross-sections after 4 MPa of reservoir pressure decrease during the production life of the reservoir. In this case, the minimum values of $SSR_{fracturing}$ and $SSR_{reactivation}$ are, respectively, 5.240 and 2.507 for the entire model domain. These values show that that it is unlikely that pressure changes during production history had led to rock failure or fault reactivation.

Similar analyses were performed for the case of CO_2 injection. In this case, the maximum pressure change within the reservoir is roughly 2 MPa. Figure 13 shows the distribution of strength-stress ratio for fracturing ($SSR_{fracturing}$) and fault reactivation ($SSR_{reactivation}$) for the north-south and east-west cross-sections. In this case, the minimum values of $SSR_{fracturing}$ and $SSR_{reactivation}$ are, respectively, 5.240 and 2.528 for the entire model domain. These values indicate that, similarly to the production case, pressure changes caused by CO_2 injection are not likely to induce rock fracturing or fault reactivation.

More specifically, as shown in Appendix D, the values of strength-stress ratio in the caprocks (i.e., the Calmar and Ireton Formations) during both production and injection scenarios show no likelihood of rock fracturing or fault reactivation as results of pressure change.

A review of the deformations predicted by the 3D geomechanical model shows that, at the end of the CO_2 injection period, the reservoirs experience a maximum vertical expansion of about 7 mm and the maximum predicted magnitude of surface heave is about 2.5 mm occurring in the central part of the reservoir (Figure 14). The lower value of maximum surface heave in comparison to the maximum reservoir's expansion demonstrates the significant effects of high overburden thickness and limited lateral extension of the reservoirs in the model.

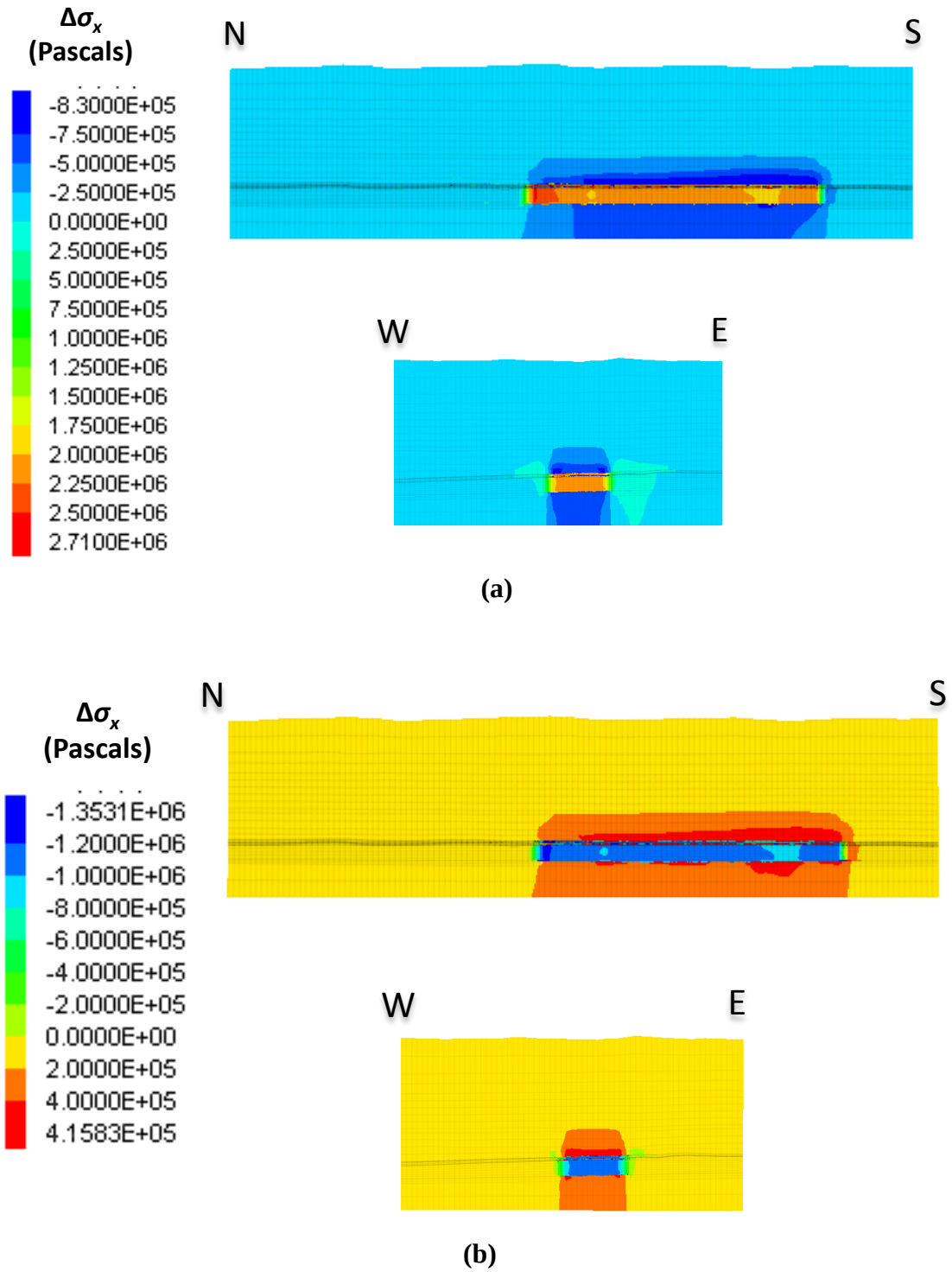

Figure 9: Distribution of induced total stress change in x direction after (a) production and (b) injection for the W-E and N-S cross-sections shown in Figure 3. The vertical scale has been exaggerated.

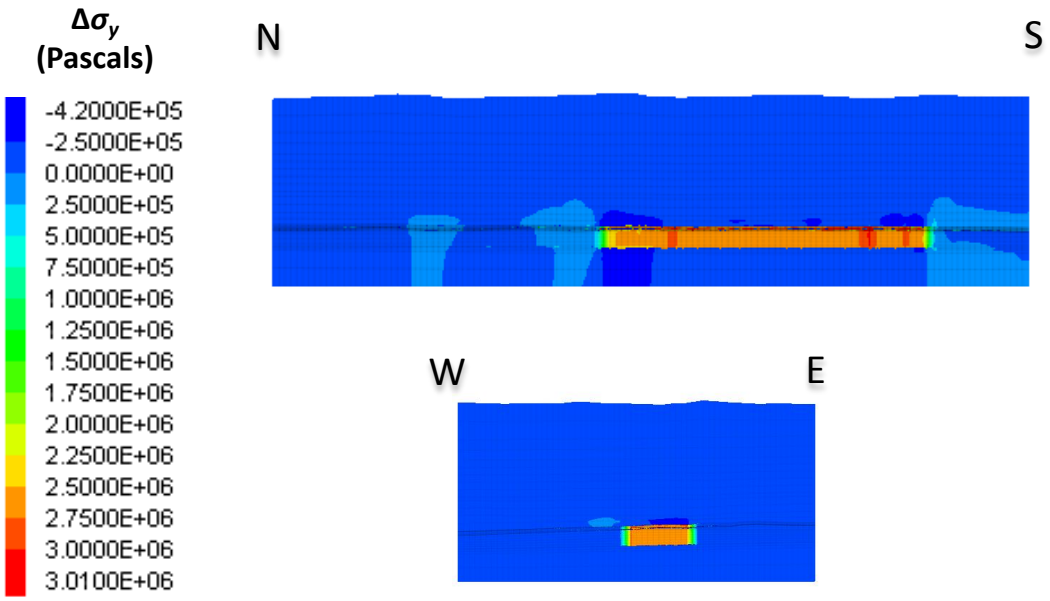

(a)

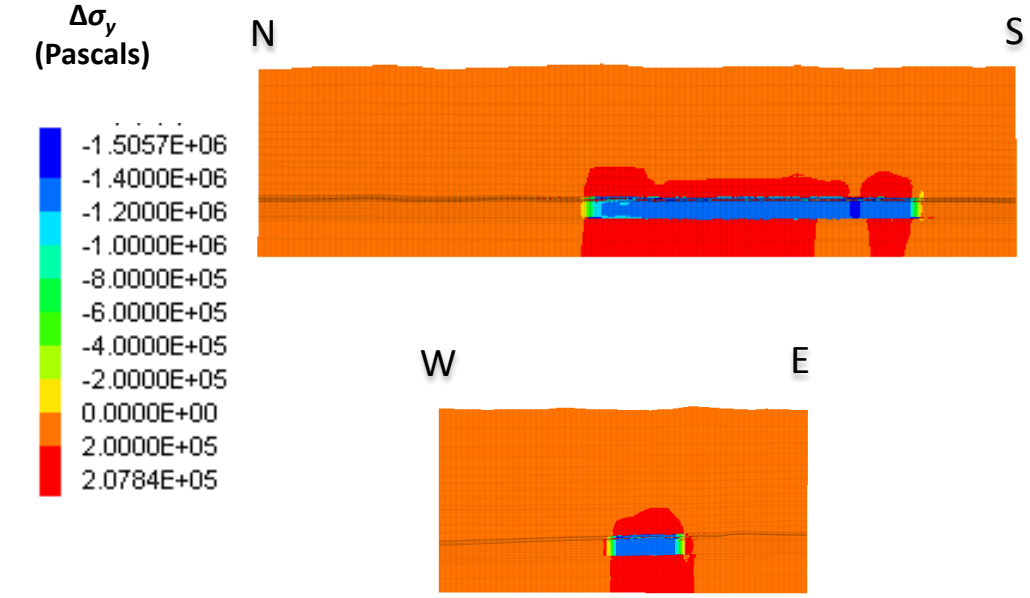

(b)

Figure 10: Distribution of induced total stress change in y direction after (a) production and (b) injection for the N-S and W-E cross-sections shown in Figure 3. The vertical scale has been exaggerated.

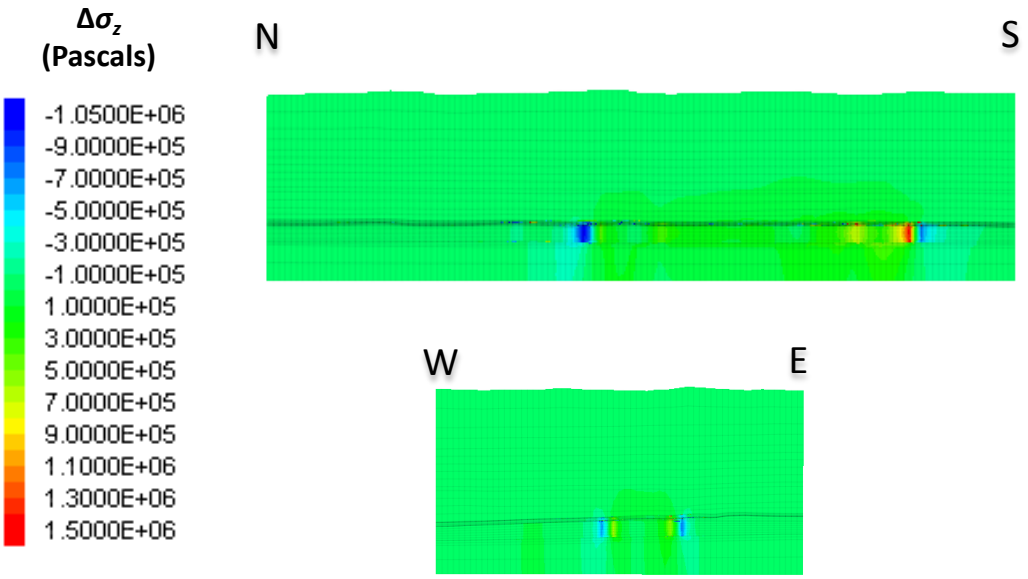

(a)

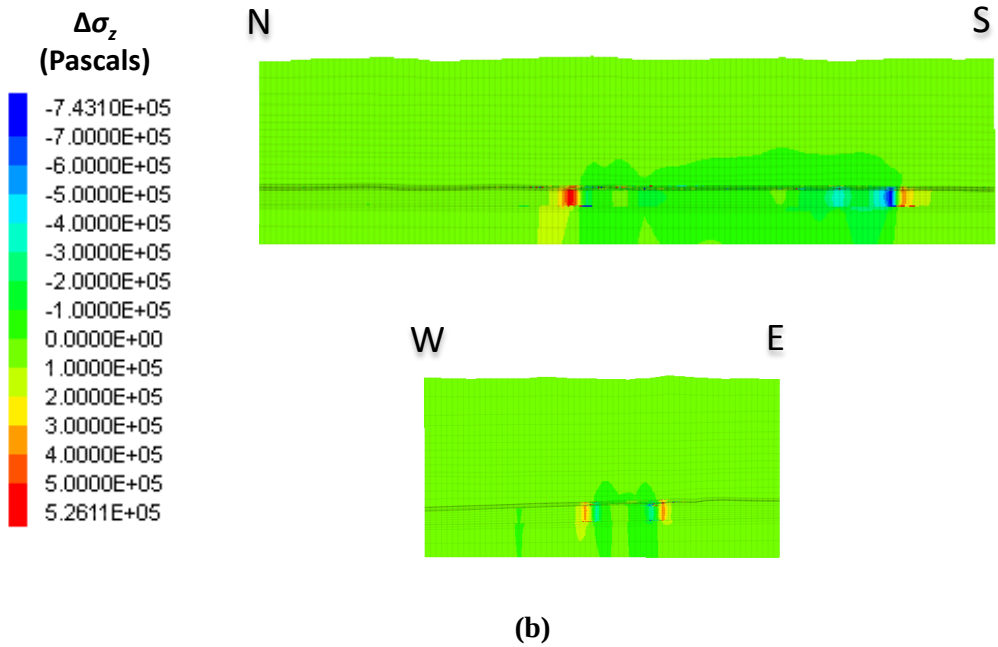

(b)

Figure 11: Distribution of induced total stress change in the vertical (z) direction after (a) production and (b) injection for the N-S and W-E cross-sections shown in Figure 3. The vertical scale has been exaggerated.

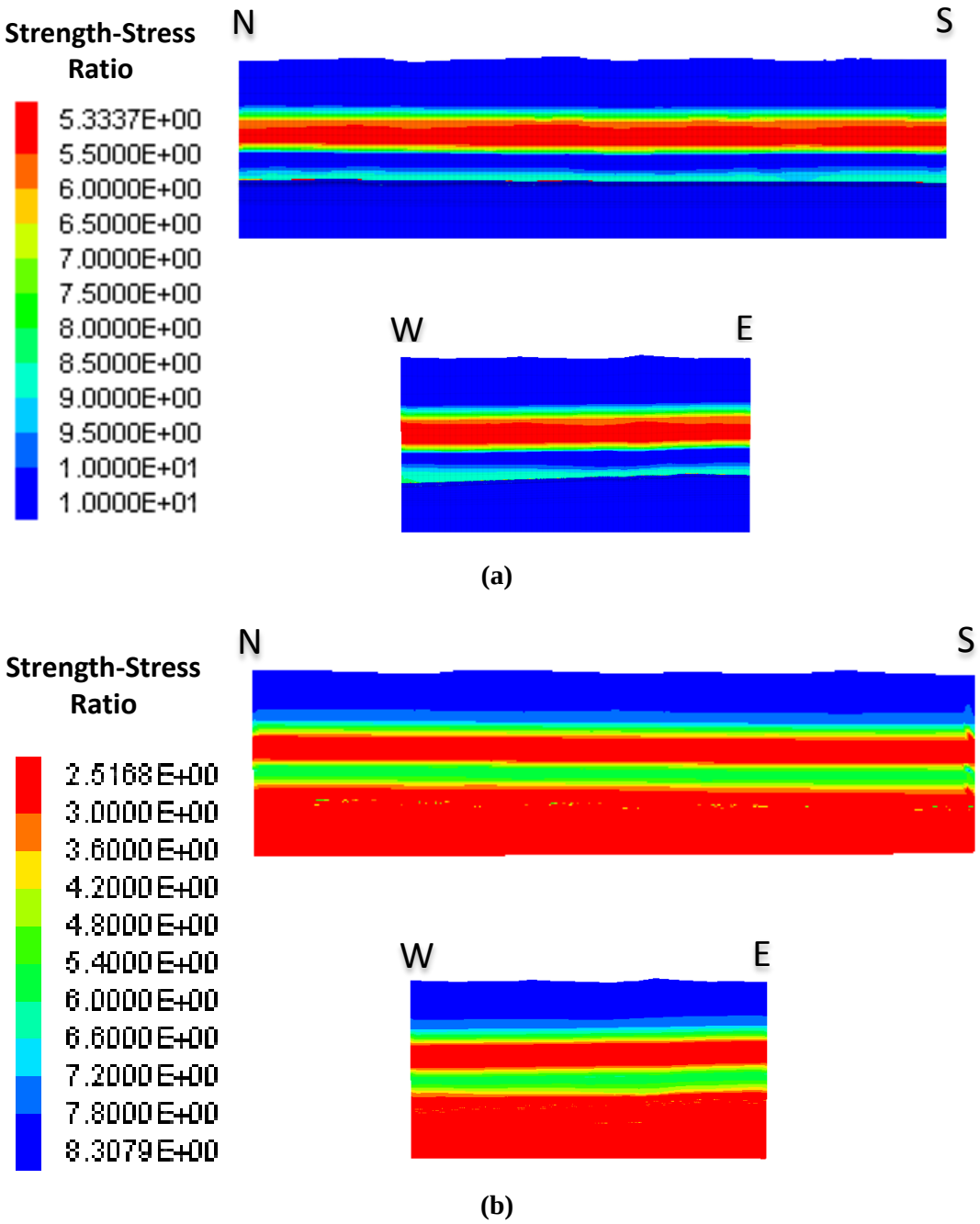

Figure 12: Distribution of strength-stress ratios (a) $SSR_{fracturing}$ (b) $SSR_{reactivation}$ after production for the N-S and W-E cross-sections shown in Figure 3. The vertical scale has been exaggerated.

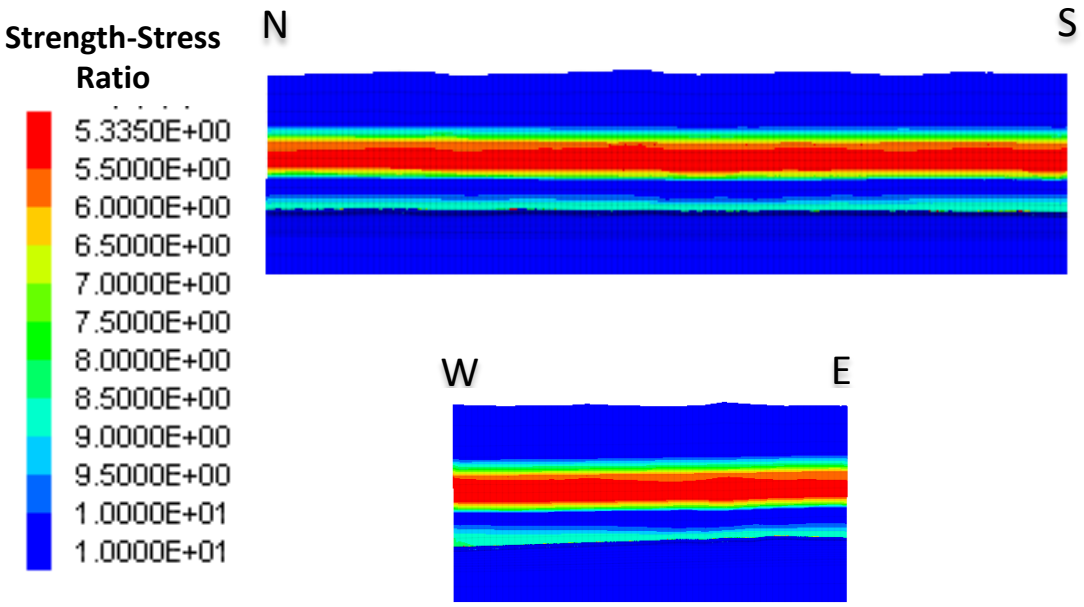

(a)

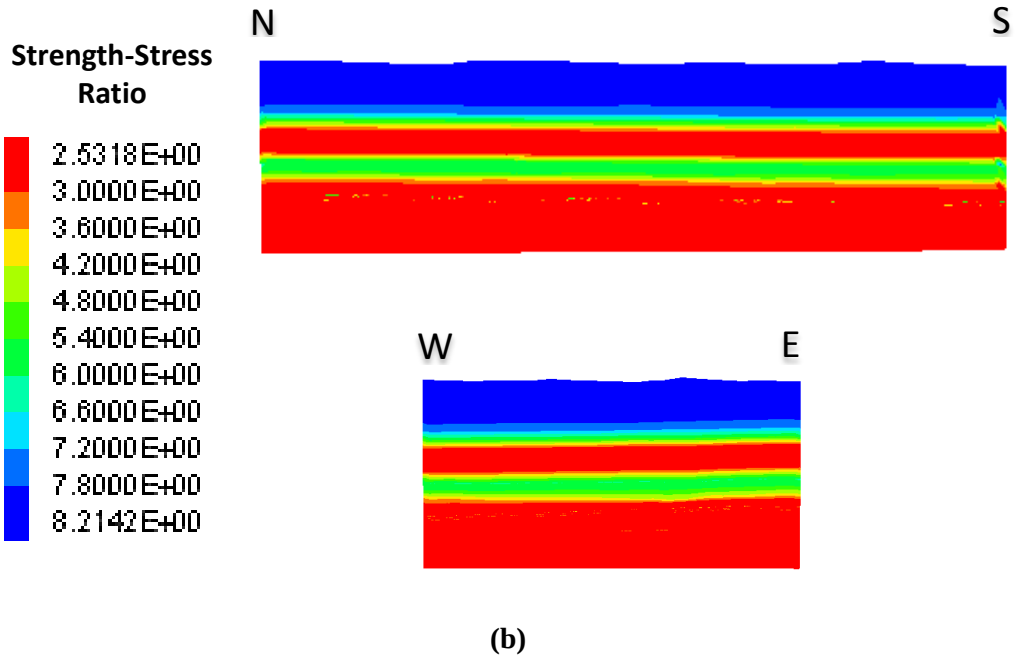

(b)

Figure 13: Distribution of strength-stress ratios (a) $SSR_{fracturing}$ (b) $SSR_{reactivation}$ after CO_2 injection for the N-S and W-E cross-sections shown in Figure 3. The vertical scale has been exaggerated.

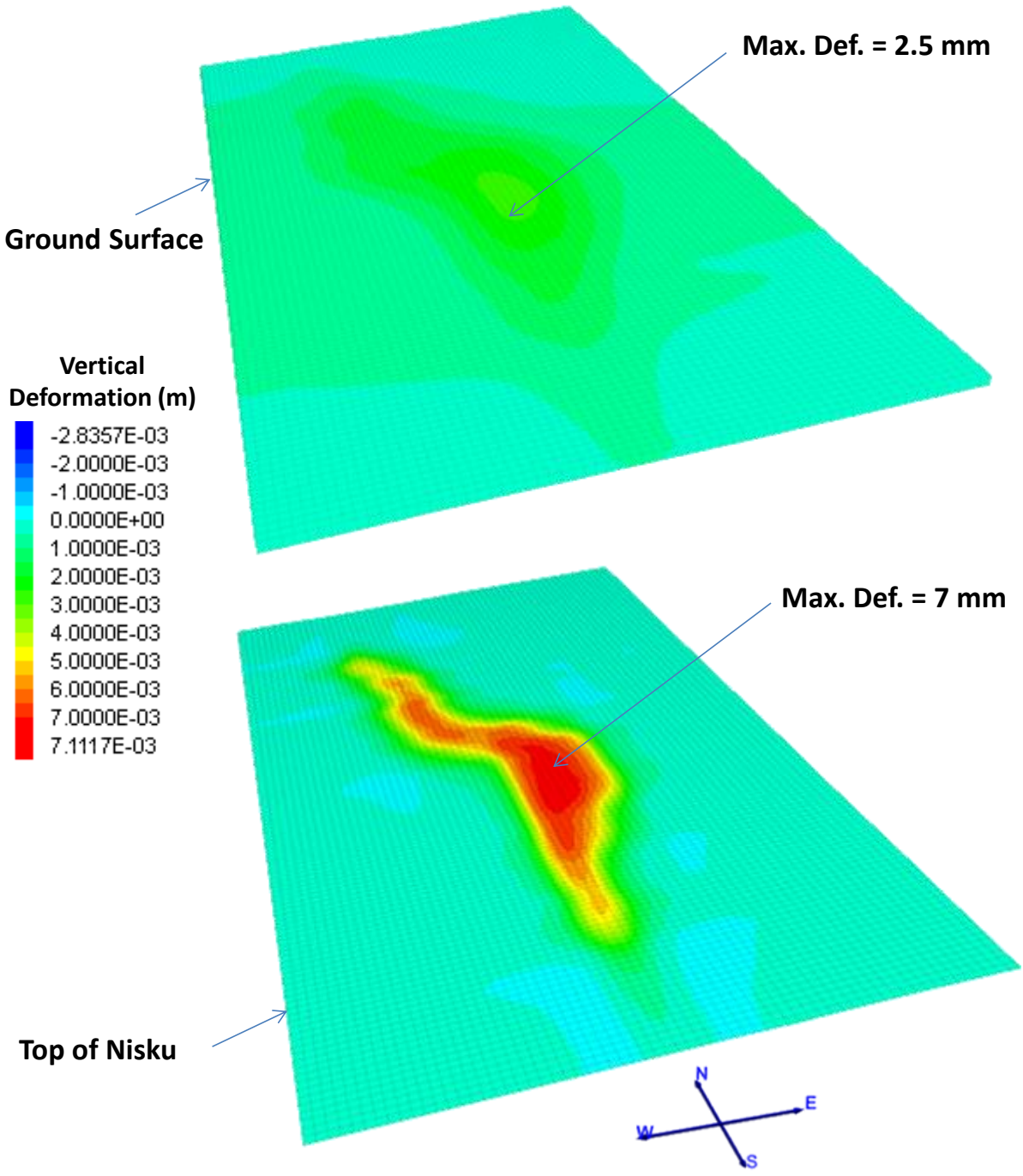

Figure 14: Distribution of vertical deformation (in meters) at the top surface of Nisku and ground surface.

4.3 Sensitivity Analysis

Uncertainties in rock mechanical properties, including elastic and strength properties, can be a major challenge in geomechanical modeling. In the following, the results of sensitivity analyses performed to evaluate the effects of variations in these properties on the geomechanical modeling are presented.

Since a linear Coulomb criterion was used in this study, the strength-stress ratios (*SSR*s) have a linear relationship with rock strength properties (i.e., cohesion and internal friction coefficient, $\mu=\tan\phi$). For instance, a 20% decrease in these values leads to the same percentage of decrease in *SSR*s. Given that the values of minimum *SSR*s from the model are significantly higher than one, there will be a reasonable margin of safety even if the rock strength parameters had been overestimated.

Sensitivity studies for uncertainties in Poisson's ratios show that for the scenario of CO_2 injection, variation of ±0.05 in the values in Poisson's ratios of the geomechanical units results in no more than 15% variation in induced stress changes. This variation has a minor effect on strength-stress ratios considering that induced stress changes are relatively small in comparison with *in-situ* stresses. Sensitivity studies for uncertainties in Young's modulus show that the induced stress changes are not sensitive to the variations in this parameter.

Figures 15(a) and 15(b) show the effects of variations in Poisson's ratios and Young's modulus on the maximum reservoir expansion and surface heave induced by CO_2 injection. As expected, these deformations are highest when both of these elastic parameters have their minimum values. From these results, for the lower values of these parameters, the maximum vertical expansion of the reservoir is less than 10 mm and the maximum surface heave is less than 5 mm.

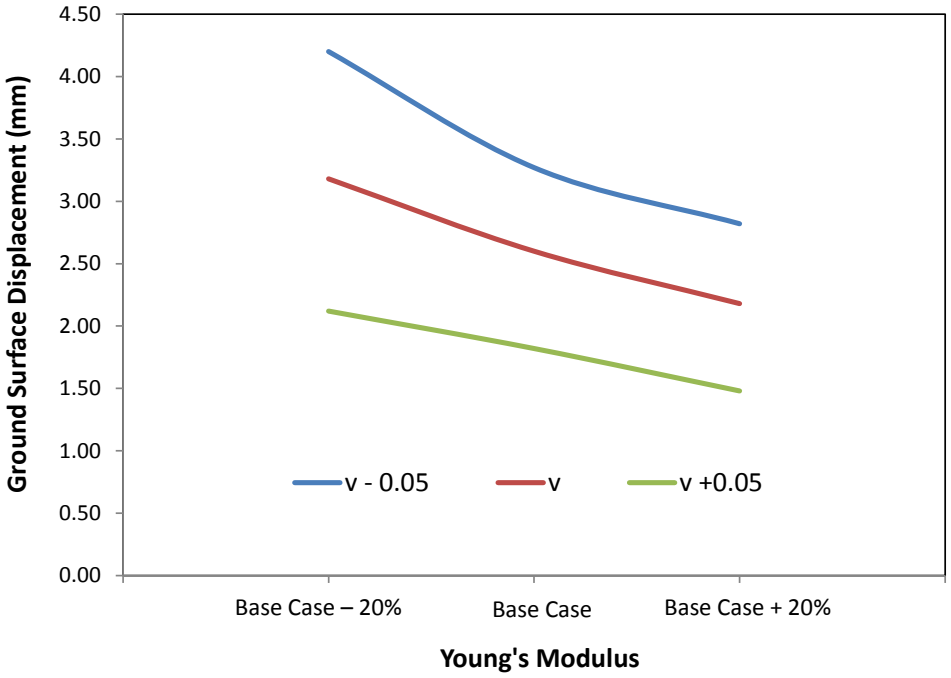

(a)

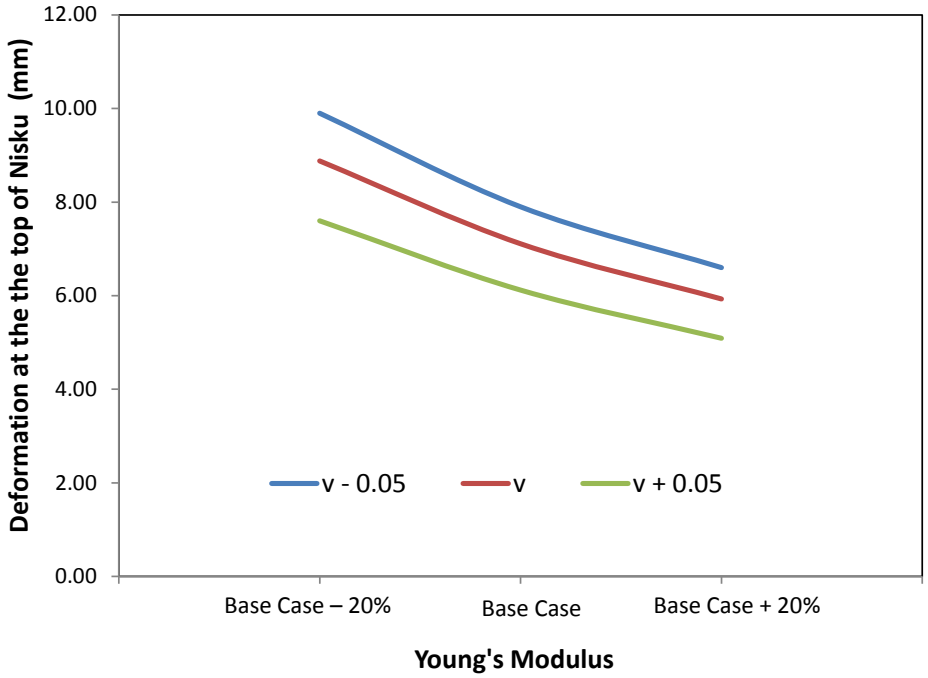

(b)

Figure 15: Sensitivity of (a) maximum ground surface heave and (b) maximum deformation at the top of Nisku to variations in Poisson's ratio and Young's modulus.

4.4 Geomechanical Analysis of Temperature Changes

As described in section 3.4, temperature changes induced by CO_2 injection for this project were predicted by a simple homogeneous single-well thermal simulation. The results of this simulation suggest that, due to the limited area affected by temperature change, a single-well model may also be used for geomechanical analysis. Therefore, a geomechanical model with a representative injection well (Figure 8) in the centre was constructed. This model covers an area of 4x4 km^2 and has a grid resolution of 50 x 50 m^2 and includes 262,400 brick (i.e., octahedron) zones (Figure 16). Other properties of this model, such as stratigraphic units and their geomechanical properties are described in Chapter 3 and are similar to the full-scale model developed for pressure-change analysis.

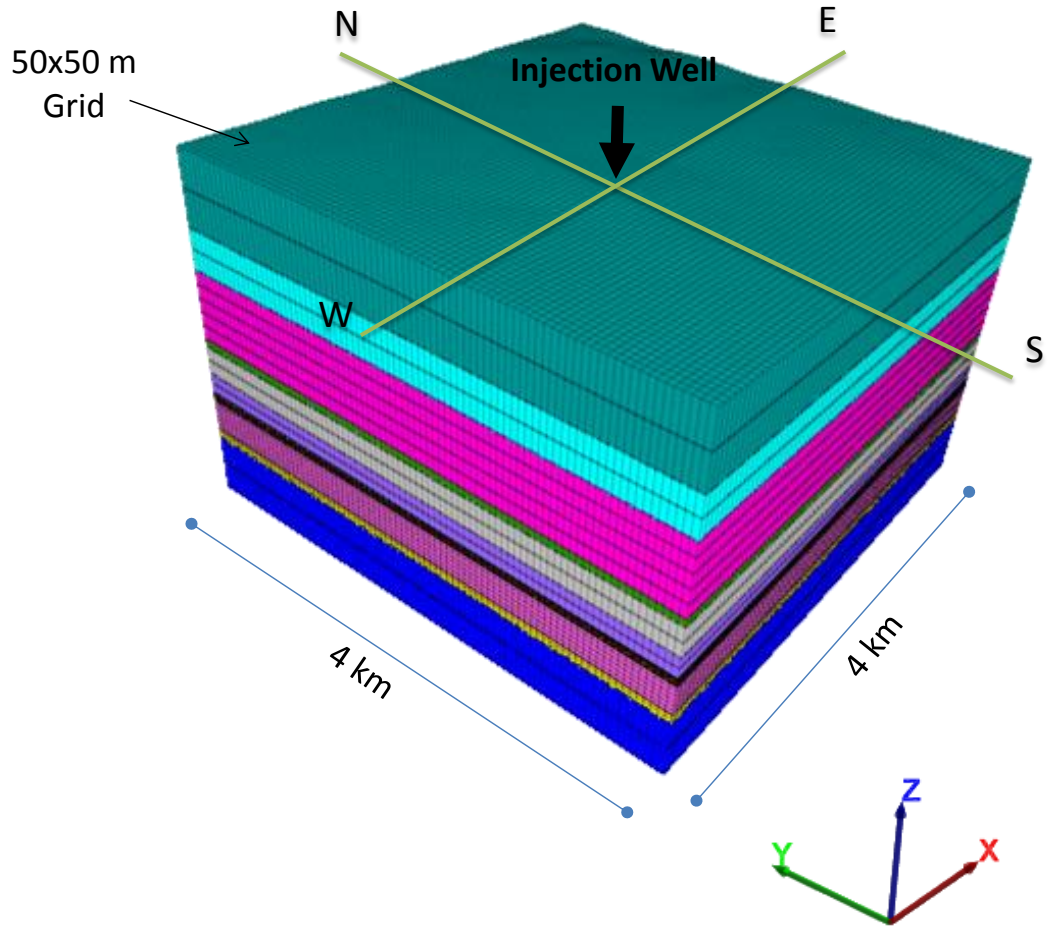

Figure 16: Three dimensional perspective view of the single-well model developed for geomechanical analysis of temperature changes using FLAC3D (Itasca Consulting Group, 2009). The vertical scale has been exaggerated.

Figure 17 shows the distribution of predicted induced stress changes in the model domain for the north-south cross section shown in Figure 16 when the injected CO_2 has a bottomhole temperature of 15°C. Figure 18 shows similar results for the scenario of injected CO_2 temperature of 30°C. For both scenarios the induced horizontal stress changes within the reservoirs are higher than the pre-injection minimum effective stresses. This means that, as results of temperature change, vertical tensile fractures are likely to form within the reservoirs. The stress changes in the caprocks show no tendency towards fracturing. However, it is important to note that this continuum-mechanics model is not capable of capturing the rock behaviour after fracture initiation and propagation. In addition, potential temperature changes within the caprocks have not been considered in this model. Therefore, its prediction for stress changes within the caprocks may be unreliable. Considering the importance of caprock integrity for CO_2 sequestration projects, it is recommended that comprehensive studies of thermal effects of CO_2 injection on the integrity of caprock are conducted in a future phase of the study. These studies must include: i) coupled fluid flow and thermal simulations of CO_2 injection with realistic data for the Clive field; and ii) geomechanical modeling of fracture initiation and propagation and their effects on stress re-distribution in the caprocks.

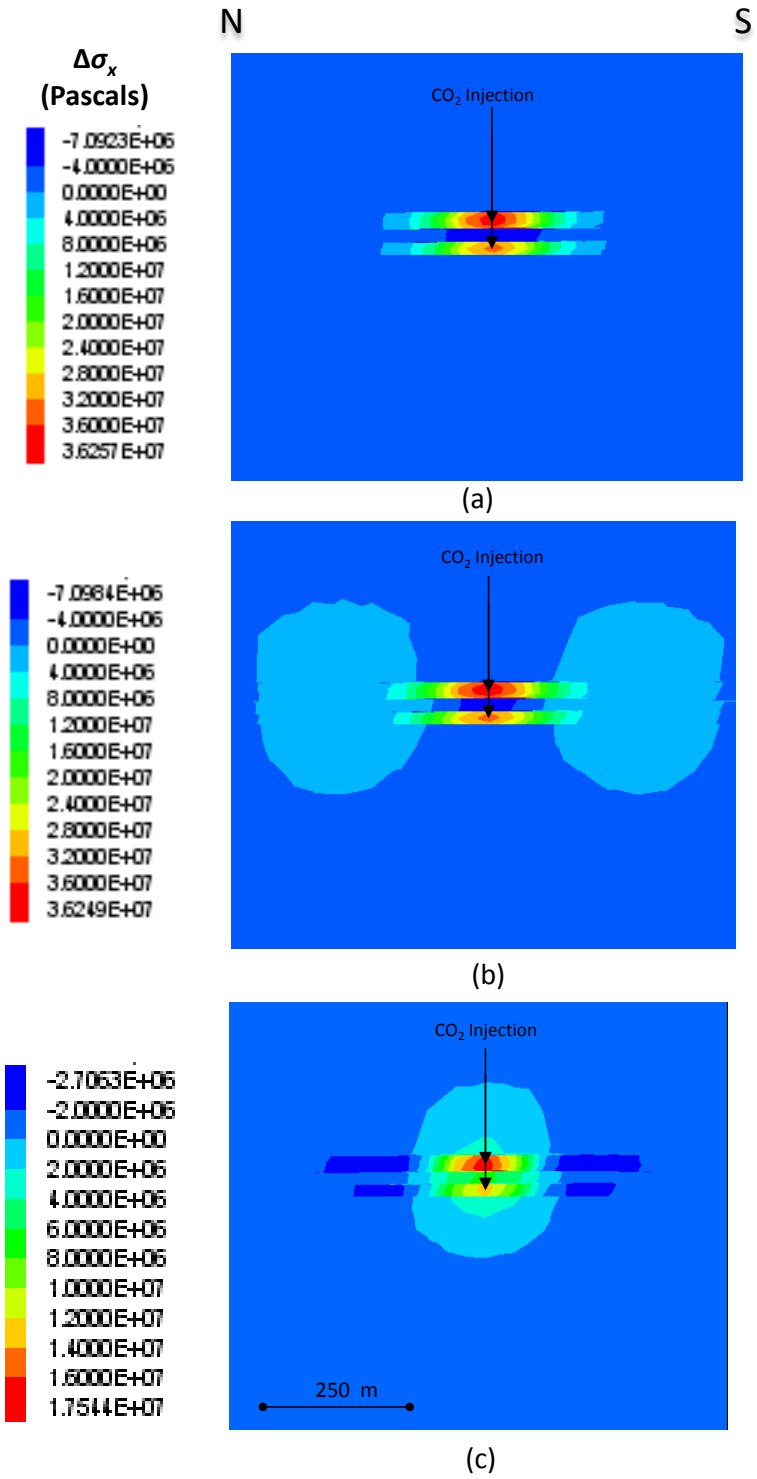

Figure 17: Distribution of induced total stress change in the (a) x direction (b) y direction and (c) z direction after 30 years of CO_2 injection with a bottomhole temperature of 15 °C for the N-S cross-section shown in Figure 16.

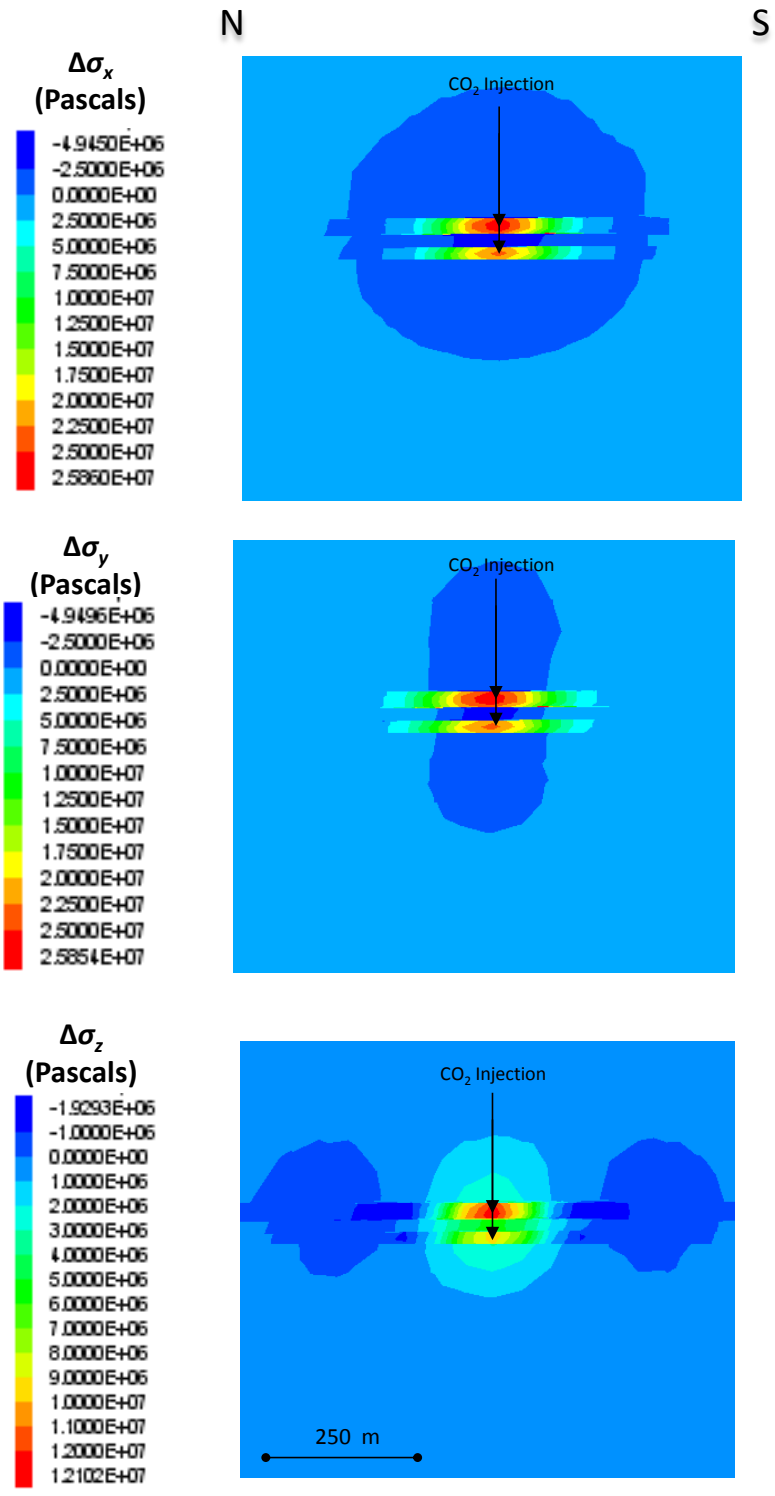

Figure 18: Distribution of induced total stress changes in the (a) x direction (b) y direction and (c) z direction after 30 years of CO_2 injection with a bottomhole temperature of 30°C for the N-S cross-section shown in Figure 16.

5. Summary and Conclusion

The developed MEM in Phase I of the project was completed by adding the stratigraphic units of interest below the Calmar Formation including the Nisku, Ireton, Leduc, and Cooking Lake formations. The geomechanical properties for these formations were calculated using log data from 16 wells within and in the vicinity of the study area.

In the first level of upscaling, an average value of each property was calculated for each stratigraphic unit in each well. Then, based on the statistical analysis of these values, it was decided that, for each property, single-value well-averages would be assigned to each stratigraphic unit in the entire study area. The reliability of this assumption was confirmed by using a series of sensitivity analyses.

A three-dimensional numerical model was developed for geomechanical analysis of the Leduc (D-3A) and Nisku (D-2) reservoirs and relevant underlying and overlying strata. The geometry of this model was derived from the geological model developed at AITF. The mechanical data for this model were derived from the developed MEM. Historical data were used to calculate the average pressure change during the production life of these reservoirs. In regard to CO_2 injection, in absence of fluid flow simulations it was assumed that the reservoir pressure will increase by 2 MPa as a result of CO_2 injection. Simple single-well thermal simulations were performed to predict temperature changes induced by CO_2 injection. A linear elastic constitutive model was used along with the Coulomb failure criterion to identify the potential for fracturing and fault reactivation.

For the case of pressure changes, the results indicate no likelihood for induced fracturing and fault reactivation within the study area for both scenarios of historical production and CO_2 injection. The results of modelling predict a maximum surface heave of 2.4 mm induced by CO_2 injection at the end of 30 years of operations. A series of sensitivity analyses show that, to a significant extent, variations in rock mechanical properties do not lead to induced fracturing or fault reactivation. The effect of these variations on the vertical reservoir expansion and ground surface heave is in order of millimetres.

A single-well geomechanical model with higher resolution geometry was developed to study the geomechanical response to temperature changes as a result of injection of cooler CO_2 into the reservoirs. The results of modelling suggest that tensile fractures are likely to occur within the reservoirs. Due to the occurrence of tensile fractures, more detailed modeling is required to study the geomechanical response of the caprock to temperature changes. It is recommended that coupled thermal-fluid flow simulations with realistic field data are conducted in a subsequent phase of the project. The results of these simulations must be used for comprehensive geomechanical studies capable of considering the effects of fracture initiation and propagation in the surrounding rock.

6. References

AITF, 2011. Geological, Hydrogeological and Mineralogical Characterization of the Sedimentary Succession Overlying the Leduc (D-3A) and Nisku (D-2) Oil Reservoirs in the Clive Oil Field in Alberta. Submitted to Enhance Energy Inc.

Bachu, S., Haug, K., Michael, B.E., Buschkuehle, B.E., Adams, J.J., 2005. Deep injection of acid-gas in western Canada. In: Underground Injection Science and Technology (C-F. Tsang and J.A. Apps, eds.), Elsevier, p. 623-635.

Bell, J.S., Price, P.R., and McLellan, P.J. 1994. *In-situ* Stress in the Western Canada Sedimentary Basin; In Geological Atlas of the Western Canada Sedimentary Basin, G.D. Mossop and I. Shetsen (comps.), Calgary, Canadian Society of Petroleum Geologists and Alberta Research Council. p. 439-446.

Chang, C., Zoback, M.D., and Khaksar, A, 2006. Empirical relations between rock strength and physical properties in sedimentary rocks. Journal of Petroleum Science and Engineering. v. 51, p. 223-237.

Computer Modelling Group's (CMG) Ltd., 2010. User's Guide – Version 2010.10.

E.ON UK plc, Temperature Effects of well and reservoir, report submitted to the Department of Energy and Climate Changes (DECC) of UK. http://www.decc.gov.uk/assets/decc/11/ccs/chapter7/7.13-temperature-effects-on-well-and-reservoir.pdf

Encyclopædia Britannica, 2012. Encyclopædia Britannica Online. Encyclopædia Britannica Inc., Web. 14 Feb. <http://www.britannica.com/EBchecked/topic/505970/rock>.

geoLOGIC Systems Ltd., 2012. geoSCOUT Help, version 7.12.0.0.

Golubev, A.A., and Rabinovich, G.Y., 1976. Resultaty primeneia appartury akusticeskogo karotasa dlja predeleina proconstych svoistv gornych porod na mestorosdeniaach tverdych isjopaemych. Prikl. Geofiz. Moskva. 73, p. 109–116.

Hearn, M.R., Machel, H.G., and Rostron, B.J., 2011. Hydrocarbon breaching of a regional aquitard: The Devonian Ireton Formation, Bashaw area, Alberta, Canada. AAPG Bulletin, v. 95, No. 6, p. 1009–1037.

Itasca Consulting Group, 2009. FLAC3D User's Guide, version 4.00.32.

Kopp, A., Bielinski, A., Ebigbo, A., Class, H., Helmig, R., 2006, Numerical Investigation of Temperature Effects during the Injection of Carbon Dioxide into Brine Aquifers: Proceedings 8th Greenhouse Gas Technology Conference, Trondheim, Norway, CD-ROM.

Lal, M., 1999. Shale stability: drilling fluid interaction and shale strength. SPE Latin American and Caribbean Petroleum Engineering Conference held in Caracas, Venezuela. SPE 53356.

LMKR GeoGraphix® Discovery Suite, 2011. PRISM Help, version 500.0.2.5.

Militzer. H., and Stoll, R., 1973. Einige Beitrageder geophysics zur primadatenerfassung im Bergbau, Neue Bergbautechnik. Lipzig 3, p. 21–25.

Oar, T., Hawkes, C.D. and Soltanzadeh, H., 2011. Geomechanical Analysis of the Clive Field for CO_2 Injection Phase I- Mechanical Earth Model. Submitted to Alberta Innovates - Technology Futures.

Schlumberger Ltd., 2009. Petrel Seismic to Simulation Software. User's Manual, version 2009.2.

Soltanzadeh, H., and Hawkes, C.D., 2011. Geomechanical Analysis for the Heartland Area Redwater Project (HARP) – Phase 2. Submitted to Alberta Innovates - Technology Futures.

Woodland, D.C., and Bell, J.S., 1989. In situ stress magnitudes from mini-frac records in western Canada. The Journal of Canadian Petroleum Technology Vol. 28. No. 5. JCPT 89-05-01

7. APPENDIX A – Calculation of Strength Properties

Table A. 1: Strength properties for shale formations using average sonic, density, and density porosity data.

Parameter	Formula (with reference number, as assigned in Chang et al., 2006)	Original Source	Validity range	Comments by Chang et al. (2006)	Ireton
V_p (m/s)	Average value →				5714
Δt_c (μs/m)	Average value →				175
UCS	$0.77(914.4/\Delta t_c)^{2.93}$ (12)	Horsrud (2001)	Mostly high porosity Tertiary shales	- These equations provide a lower bound of UCS for shales. - These equations calibrated for samples from the Noth Sea and Gulf of Mexico where high porosity, unconsolidated Tertiary or younger shales are dominant. - these equations are good for weak shales. * **Equation (15) suggested for weak shales.**	98
UCS	$0.43(914.4/\Delta t_c)^{3.2}$ (13)	Chang et al. (2006)	Pliocene and younger		**85**
UCS	$1.35(914.4/\Delta t_c)^{2.6}$ (14)	Chang et al. (2006)	-		99
UCS	$0.5(914.4/\Delta t_c)^{3}$ (15)	Chang et al. (2006)	-		**71**
UCS	$10(914.4/\Delta t_c - 1)$ (16)	Lal (1999)	Mostly high porosity Tertiary shales		42
UCS Range					**42-99**
Suggested UCS					**78**
Suggested ϕ	$\sin^{-1}\left(\frac{V_p - 1000}{V_p + 1000}\right)$ (30)	Lal (1999)	-		**45**

Table A. 2: Strength properties for carbonate formations using logs average sonic, density, and density porosity data.

Parameter	Formula (with reference number, as assigned in Chang et al., 2006)	Original Source	Validity range	Comments by Chang et al. (2006)	Nisku	Leduc
Δt_c (μs/m)	Average value →				162	170
UCS	$(23046/\Delta t_c)^{1.82}/145$ (22)	Militizer and Stoll (1973)	-	- defines a clear lower bound ***suggested when a conservative strength estimation is important such as for a wellbore stability problem**	**57**	52
UCS	$10^{(2.44+327.42/\Delta t_c)}/145$ (23)	Golubev and Rabinovish (1976)	-	- statistically it is more favourable than (22)	199	160
UCS Range					57-199	52-160
Suggested UCS					**199**	**160**

8. APPENDIX B – Calculation of Elastic Properties

Data			
UWI	Ed (MPa) for Nisku	Ed (MPa) for Ireton	Ed (MPa) for Leduc
100/03-20-040-25W4/00	103.0	72.5	60.2
100/06-14-038-24W4/00	89.7	82.7	63.4
100/09-03-039-24W4/00	90.1	71.6	79.8
100/10-22-039-23W4/02	95.2	79.7	86.4
100/11-19-040-24W4/00	96.5	65.9	82.9
100/14-05-041-24W4/00	95.5	73.8	63.4
100/14-11-038-24W4/00	84.2	88.7	67.8
100/14-34-038-24W4/00	93.2	83.7	88.6
100/15-15-038-24W4/00	87.2	90.4	78.8
100/16-08-041-24W4/00	101.2	70.5	87.9
100/16-11-038-24W4/00	91.9	87.6	74.0
100/16-15-038-24W4/00	81.4	77.7	73.8
102/10-02-039-23W4/00	93.0	79.3	86.8
103/01-27-038-24W4/00	94.3	81.4	77.9
Statistical Analysis			
Number of Data	14	14	14
Minimum Value	81.4	65.9	60.2
Maximum Value	103.0	90.4	88.6
Average	92.6	79.0	76.6
Standard Deviation	5.9	7.4	9.8
Relative Std. Dev. (%)	6	9	13

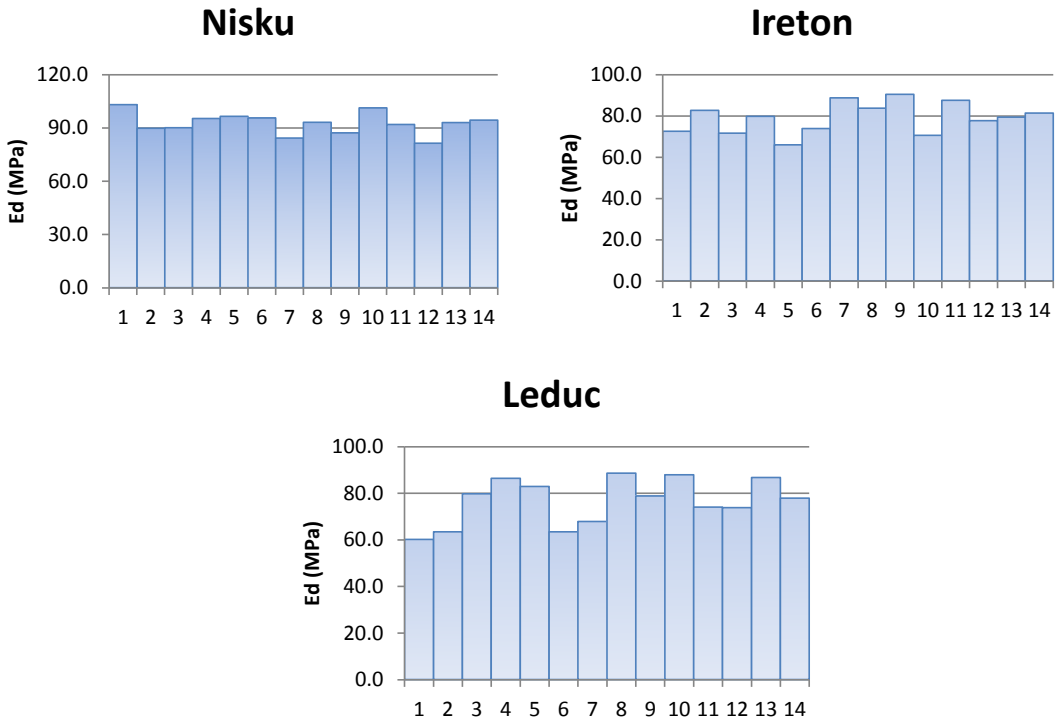

Figure B. 1: The table includes average dynamic Young's moduli (E_d) from well log analysis and their statistical analysis for each stratigraphic unit. The histograms show variations of these values.

Data			
UWI	Sv Gradient (kPa/m) for Nisku	Sv Gradient (kPa/m) for Ireton	Sv Gradient (kPa/m) for Leduc
100/03-20-040-25W4/00	23.6	23.7	23.8
100/06-14-038-24W4/00	23.7	23.8	23.8
100/07-03-038-24W4/00	23.6	23.6	23.7
100/09-03-039-24W4/00	23.1	23.1	23.2
100/10-22-039-23W4/02	22.9	23.0	23.0
100/11-19-040-24W4/00	23.6	23.7	23.7
100/14-05-038-23W4/00	23.9	23.9	_
100/14-05-041-24W4/00	23.1	23.2	23.2
100/14-11-038-24W4/00	23.3	23.3	23.3
100/14-34-038-24W4/00	22.9	22.9	23.0
100/15-15-038-24W4/00	23.6	23.6	23.6
100/15-29-041-23W4/00	23.3	23.3	23.4
100/16-08-041-24W4/00	23.7	23.8	23.8
100/16-11-038-24W4/00	23.8	23.8	23.9
100/16-15-038-24W4/00	22.9	23.0	23.0
102/08-10-038-24W4/00	_	_	_
103/01-27-038-24W4/00	23.1	23.2	23.2
104/10-15-038-24W4/00	_	_	_
Statistical Analysis			
Number of Data	16	16	15
Minimum Value	22.9	22.9	23.0
Maximum Value	23.9	23.9	23.9
Average	23.4	23.4	23.4
Standard Deviation	0.3	0.3	0.3
Relative Std. Dev. (%)	1	1	1

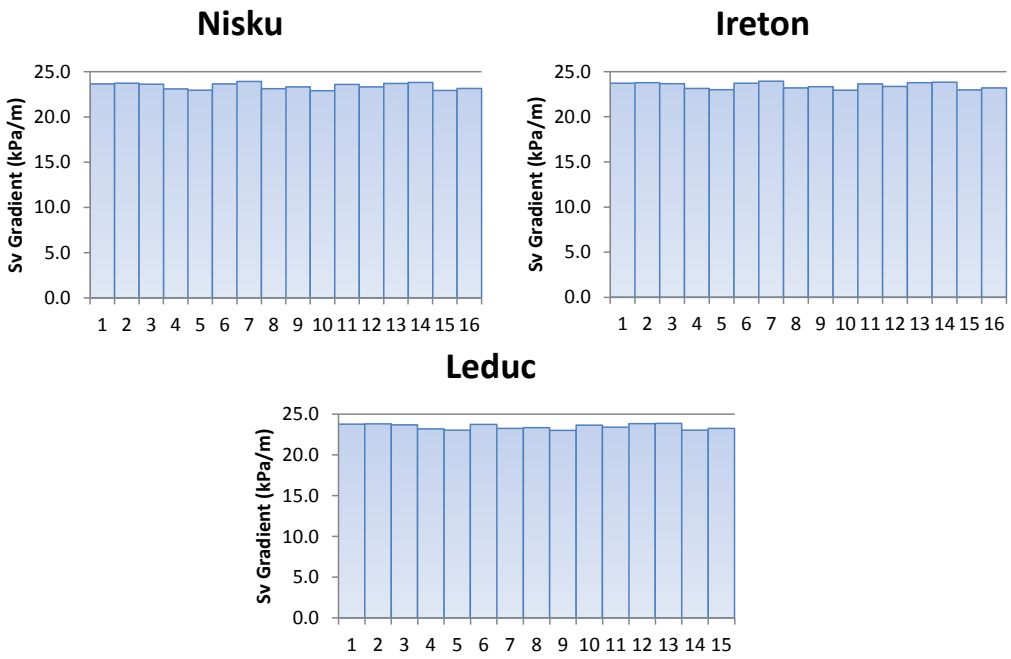

Figure B. 2: The table includes average gradientes of vertical *in-situ* stress (S_v) from well log analysis and their statistical analysis for each stratigraphic unit. The histograms show variations of these values.

Data			
UWI	Shmin Gradient (kPa/m) for Nisku	Shmin Gradient (kPa/m) for Ireton	Shmin Gradient (kPa/m) for Leduc
100/03-20-040-25W4/00	19.6	18.3	17.9
100/06-14-038-24W4/00	19.4	19.4	18.6
100/07-03-038-24W4/00	16.0	16.0	16.0
100/09-03-039-24W4/00	19.2	18.4	19.4
100/10-22-039-23W4/02	19.8	19.2	20.1
100/11-19-040-24W4/00	19.5	18.1	19.6
100/14-05-038-23W4/00	18.9	_	_
100/14-05-041-24W4/00	19.4	18.6	18.3
100/14-11-038-24W4/00	19.0	19.6	18.8
100/14-34-038-24W4/00	19.3	19.1	19.9
100/15-15-038-24W4/00	19.2	19.8	19.5
100/16-08-041-24W4/00	19.9	18.5	20.0
100/16-11-038-24W4/00	19.5	19.7	19.3
100/16-15-038-24W4/00	18.6	18.8	19.0
103/01-27-038-24W4/00	19.4	19.1	19.3
Statistical Analysis			
Number of Data	15	14	14
Minimum Value	16.0	16.0	16.0
Maximum Value	19.9	19.8	20.1
Average	19.1	18.8	19.0
Standard Deviation	0.9	1.0	1.1
Relative Std. Dev. (%)	5	5	6

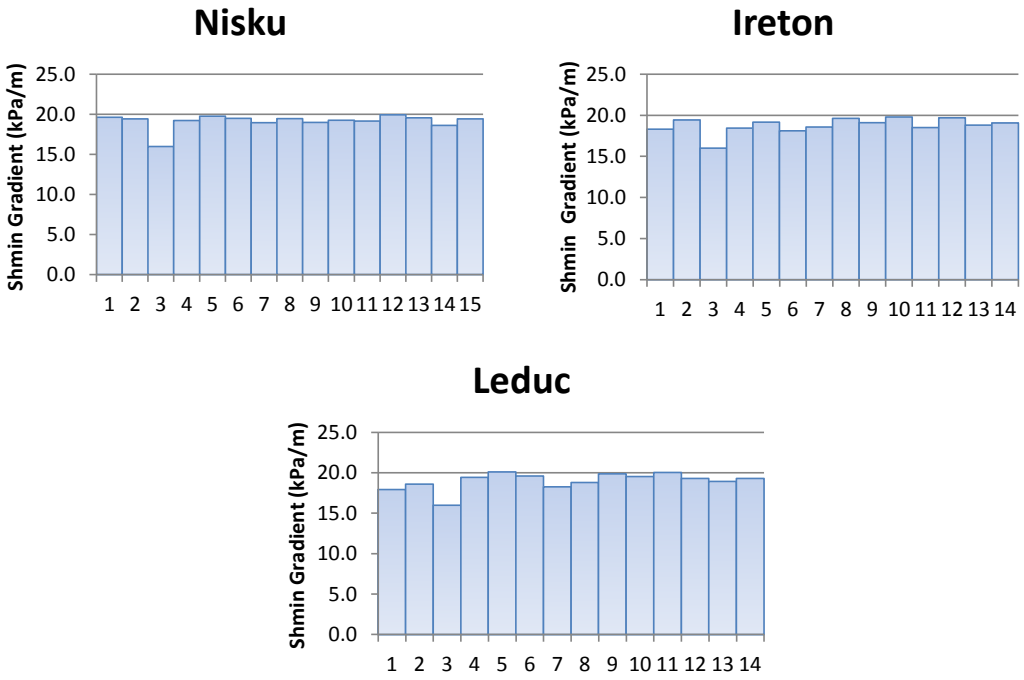

Figure B.3: The table includes average gradientes of minimum horizontal *in-situ* stress (S_{hmin}) from well log analysis and their statistical analysis for each stratigraphic unit. The histograms show variations of these values.

Data			
UWI	SHmax Gradient (kPa/m) for Nisku	SHmax Gradient (kPa/m) for Ireton	SHmax Gradient (kPa/m) for Leduc
100/03-20-040-25W4/00	33.0	30.6	28.3
100/06-14-038-24W4/00	32.8	32.6	30.5
100/07-03-038-24W4/00	32.1	32.3	32.1
100/09-03-039-24W4/00	32.8	32.1	32.8
100/10-22-039-23W4/02	33.0	33.0	33.0
100/11-19-040-24W4/00	33.0	30.1	32.5
100/14-05-038-23W4/00	32.9	_	_
100/14-05-041-24W4/00	32.8	31.3	29.9
100/14-11-038-24W4/00	32.1	33.0	30.7
100/14-34-038-24W4/00	32.9	32.9	32.8
100/15-15-038-24W4/00	32.8	33.0	32.8
100/16-08-041-24W4/00	33.0	31.0	32.7
100/16-11-038-24W4/00	33.0	33.0	32.7
100/16-15-038-24W4/00	32.3	32.4	32.2
103/01-27-038-24W4/00	33.0	32.6	32.2
Statistical Analysis			
Number of Data	15	14	14
Minimum Value	32.1	30.1	28.3
Maximum Value	33.0	33.0	33.0
Average	32.8	32.1	31.8
Standard Deviation	0.3	1.0	1.4
Relative Std. Dev. (%)	1	3	4

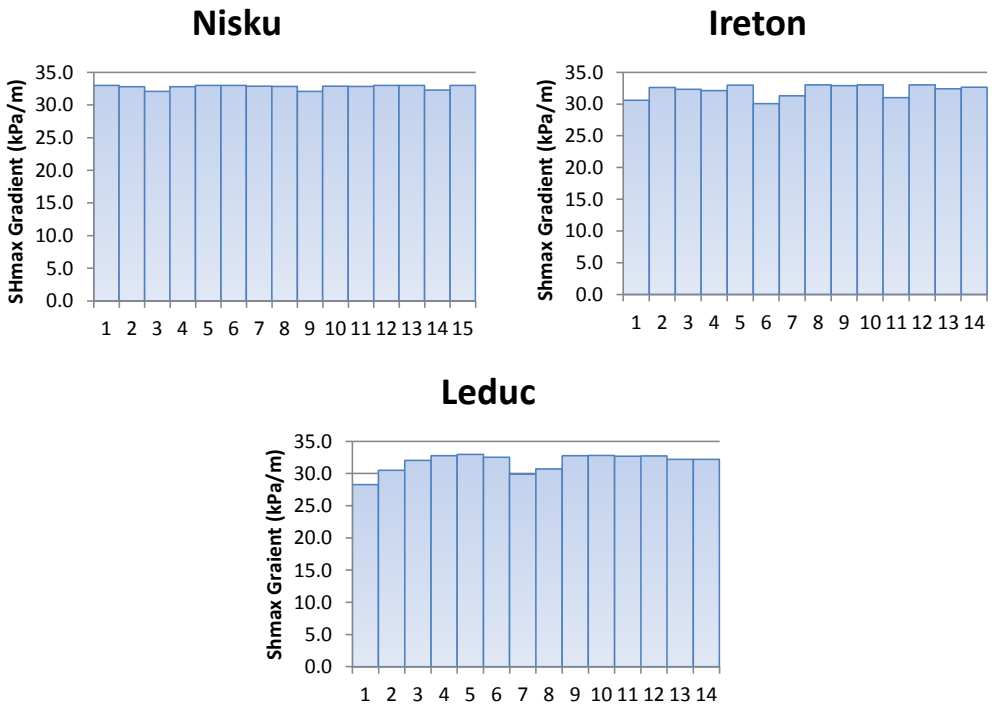

Figure B-4. The table includes average gradientes of minimum horizontal *in-situ* stress (S_{Hmax}) from well log analysis and their statistical analysis for each stratigraphic unit. The histograms show variations of these values.

9. APPENDIX C – Thermal Simulation

One of the important issues associated with CO_2 injection is the temperature evolution in the target reservoir. The diffusion of the temperature perturbation triggered by the injection of cold CO_2 into the reservoir is controlled by several parameters including the enthalpy of the CO_2 (injection temperature), thermal properties (heat capacity and heat conductivity) of the rock (reservoir and surrounding formations) and fluids, coupled with the Joule-Thomson cooling effect (Kopp et al., 2006). Therefore, a single well radial model was developed to assess the non-isothermal impact associated with CO_2 injection into the Leduc (D-3A) and Nisku (D-2) reservoirs. The injection temperature is believed to be somewhere between 15°C to 30°C, compared to the reservoir temperature of about 65°C. The highest temperature difference will probably occur around the wellbore.

For this study, the Computer Modelling Group's (CMG) reservoir compositional simulator GEM® along with associated visualization programs BUILDER® and RESULTS® were used (CMG, 2010). Due to lack of any petro-physical and thermal properties data (such as porosity, permeability, fluid saturation, relative permeability, heat capacity and thermal conductivity of the native rock and fluid etc.) and fluid pressure-temperature-volume properties (PVT) data, the modelling problem was simplified such that the model was initialized with 100% water saturation and constant permeability and porosity. The parameters used to populate the developed radial-angular cylindrical model (CMG, 2010) are given in Table C.1: Parameters used to set up the reservoir simulation model.Table C.1.

To properly set up the injection operation, a number of injection constraints such as wellhead injection pressure (WHIP), wellhead injection temperature (WHIT), bottomhole injection pressure (BHIP) and bottomhole injection temperature (BHIT) are required (E.ON UK plc). No wellbore hydraulic calculations were performed simply because it was beyond the scope of this study; however, as a range of injection temperatures (15°C to 30°C) was the only parameter provided, therefore an injection pressure of 20 MPa was chosen based on the reservoir pressure of 15 MPa at the beginning of the CO_2 injection operation. It was also decided to use 30°C as the injection temperature. A radial model with three layers in vertical direction and 100 rings in horizontal direction was developed. The radius of the model is 1000 m and a CO_2 injector located at the center and completed at the third (deepest) layer (K=1 and 3 are the uppermost and lower most layers respectively). Also, an infinite outer boundary condition was defined to keep the pressure almost constant and avoid any boundary effects on the results (Figure C.1).

The results of the simulation are shown in Figure C.2

Figure C.2: as a set of temperature profiles over the entire injection period. As it can be seen, the radius of temperature influence can go as far as approximately 200 m away from the injector well during the 30 years injection period. Also the temperature fronts

seem to be converging to a maximum distance from the well. Of course, all presented results are based on the simplified homogenous model with parameters given in Table C.1; thus, for detailed and more accurate results, a realistic geological model populated with representative parameters is required.

After the cessation of CO_2 injection, the temperature around the wellbore starts to buildup (increase) and stabilize to the reservoir temperature (Figure C.3).

Table C.1: Parameters used to set up the reservoir simulation model.

Porosity	10%
Permeability (I, J, K)	20, 20, 2 mD
Water saturation	100%
Injection period	30 yrs
Injection temperature	30°C
Injection pressure	20 MPa
Surface injection rate	100,000 m3/d
Heat capacity of reservoir and surrounding formations	1046.7 J/(kg.K)
Thermal conductivity of reservoir and surrounding formations	3.461 J/(m.s.K)
Reservoir temperature	65°C
Reservoir pressure	15 MPa
Reservoir thickness	15 m
Reservoir radius	1000 m

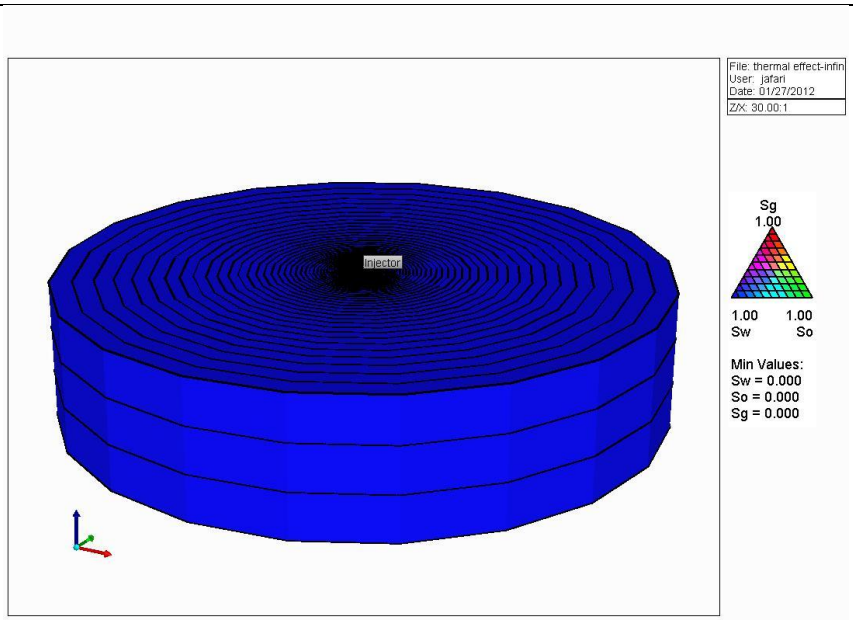

Figure C.1: A 3-D view of the developed radial model with completely water saturation.

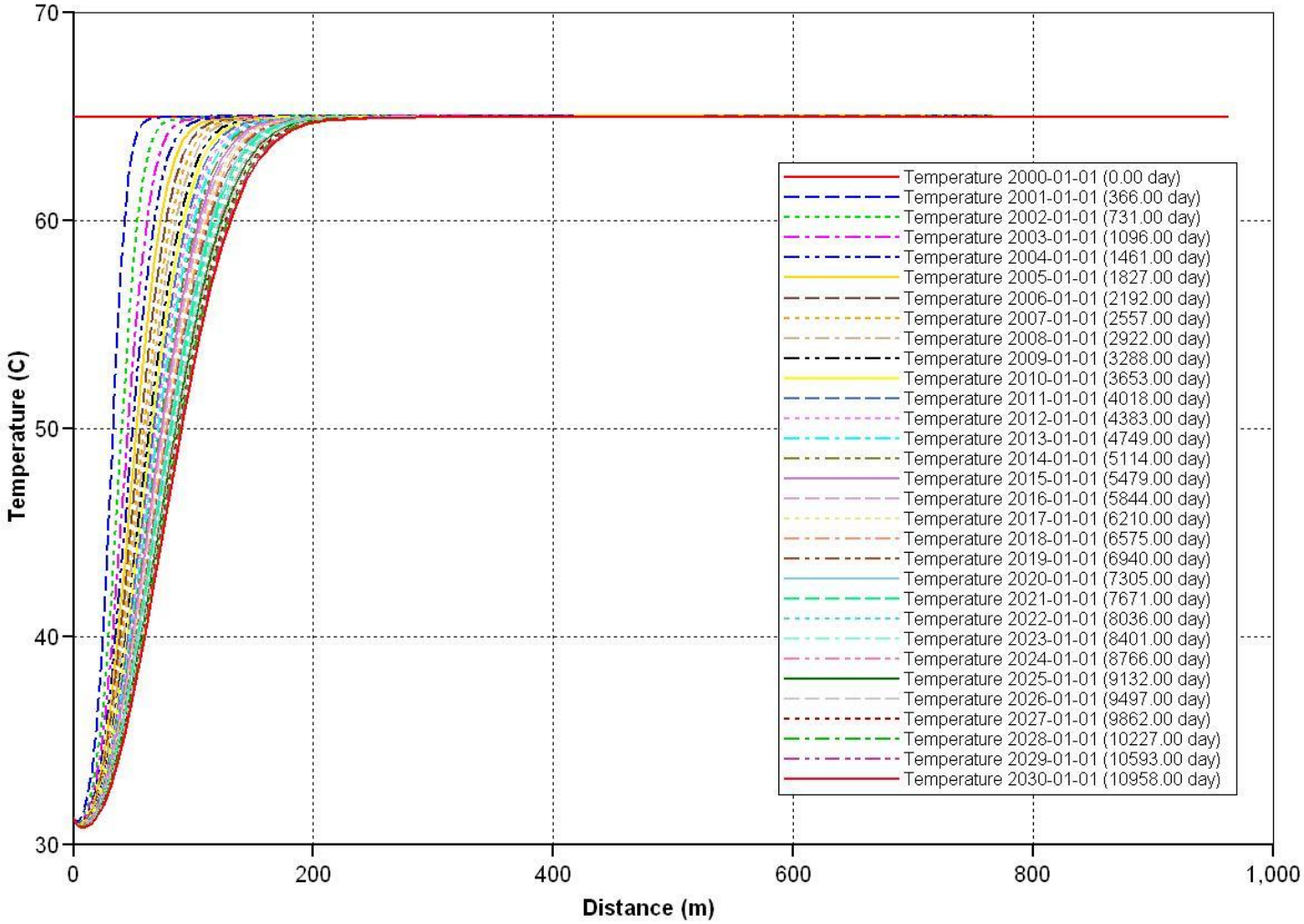

Figure C.2: The temperature profile of the simulated model.

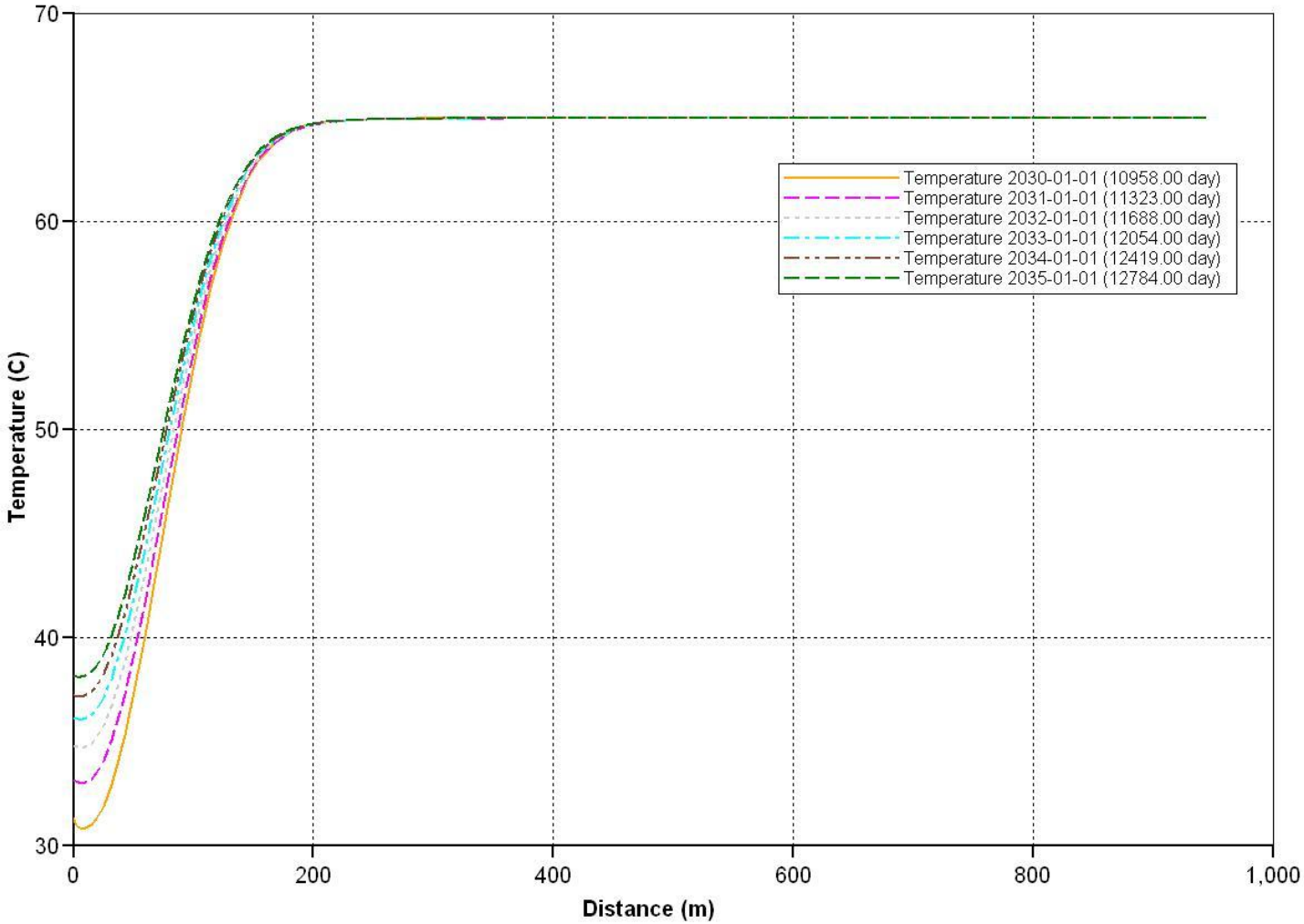

Figure C.3: Temperature build-up (increase) around the wellbore after cessation of CO_2 injection.

10. APPENDIX D – Strength-Stress Ratios for the caprocks (Ireton and Calmar)

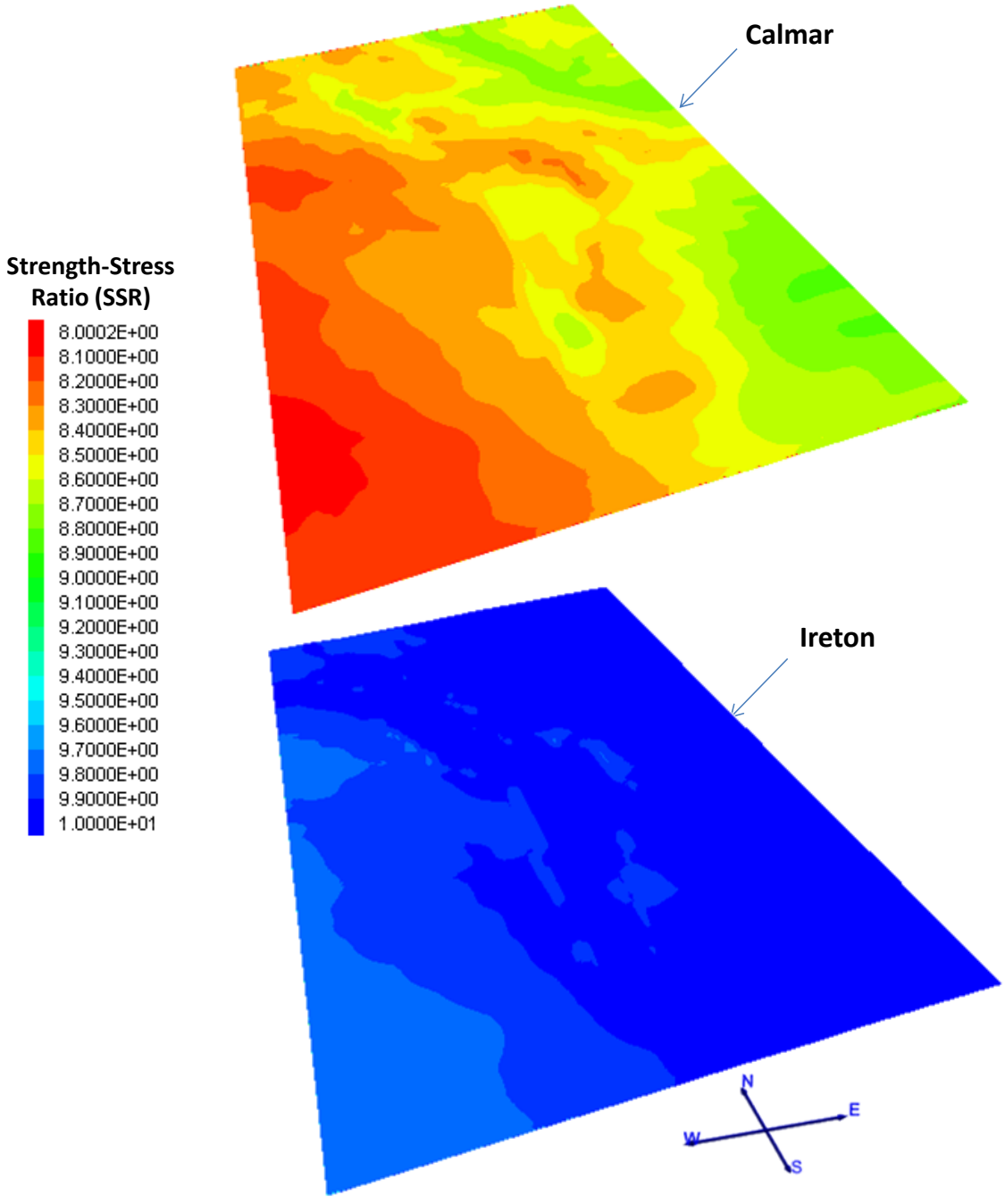

Figure D.1: Distribution of strength-stress ratio for rock fracturing ($SSR_{fracturing}$) for the Ireton and Calmar units after production.

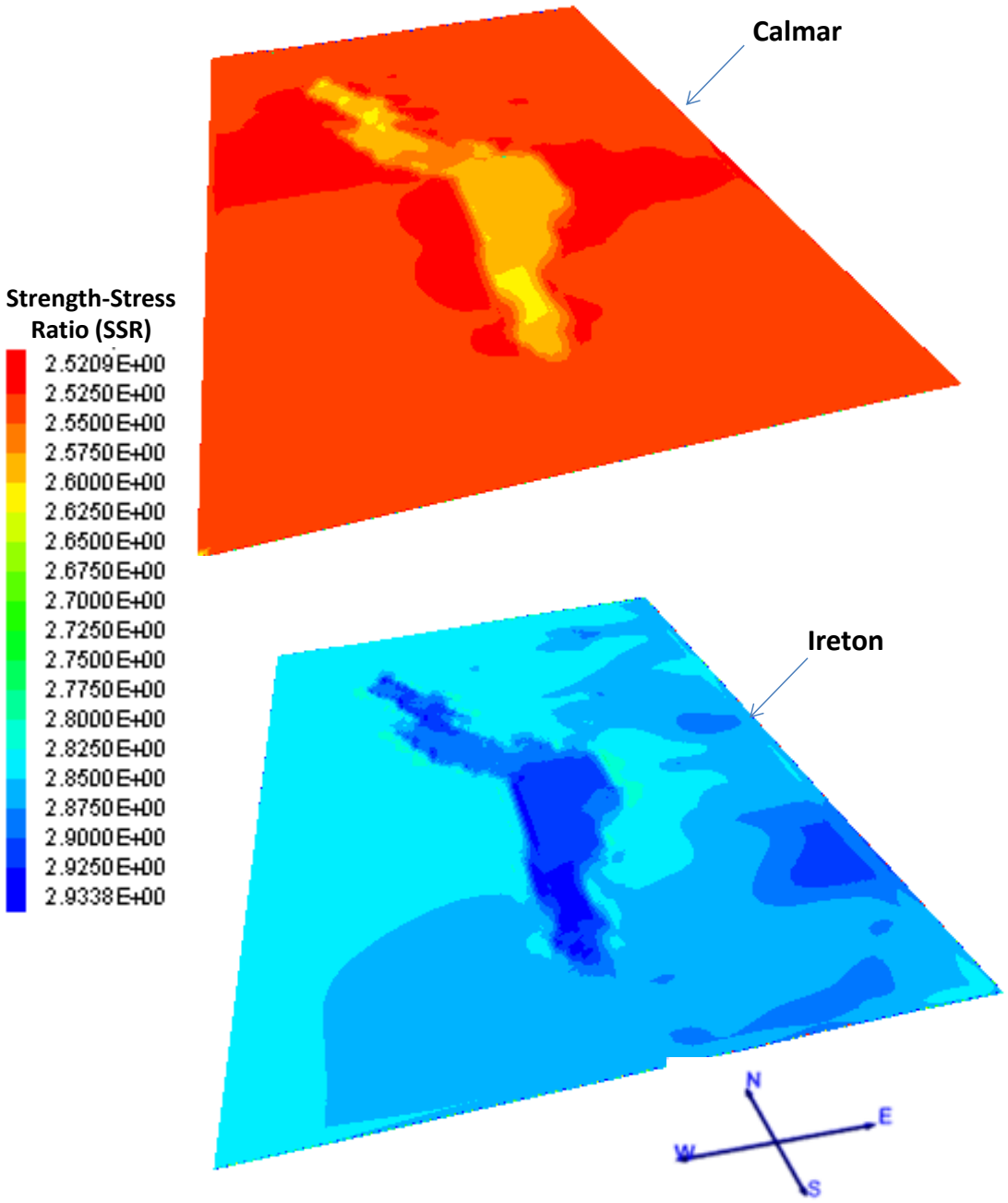

Figure D.2: Distribution of strength-stress ratio for fault reactivation ($SSR_{reactivation}$) for the Ireton and Calmar units after production.

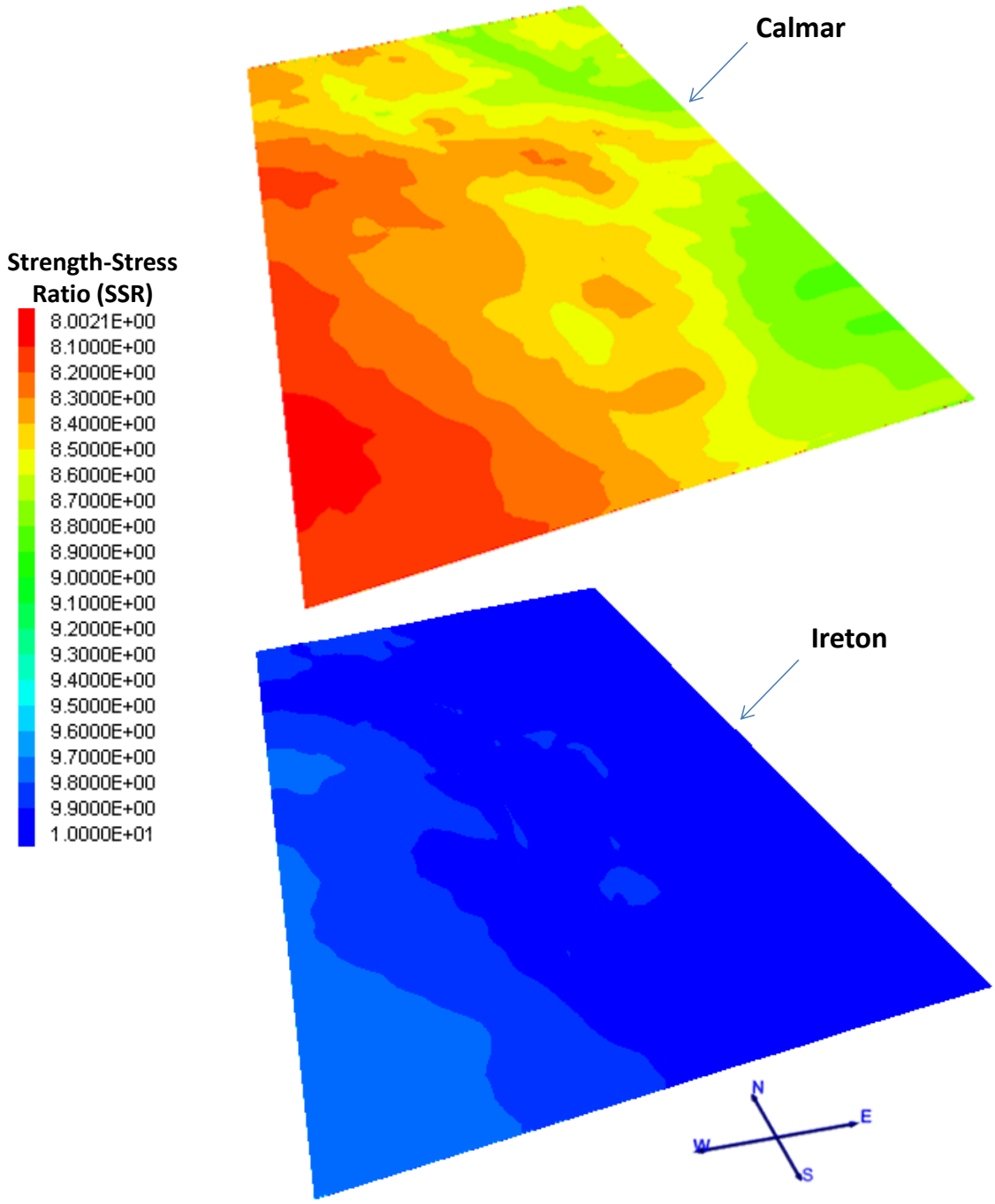

Figure D.3: Distribution of strength-stress ratio for rock fracturing ($SSR_{fracturing}$) for the Ireton and Calmar units after CO_2 injection.

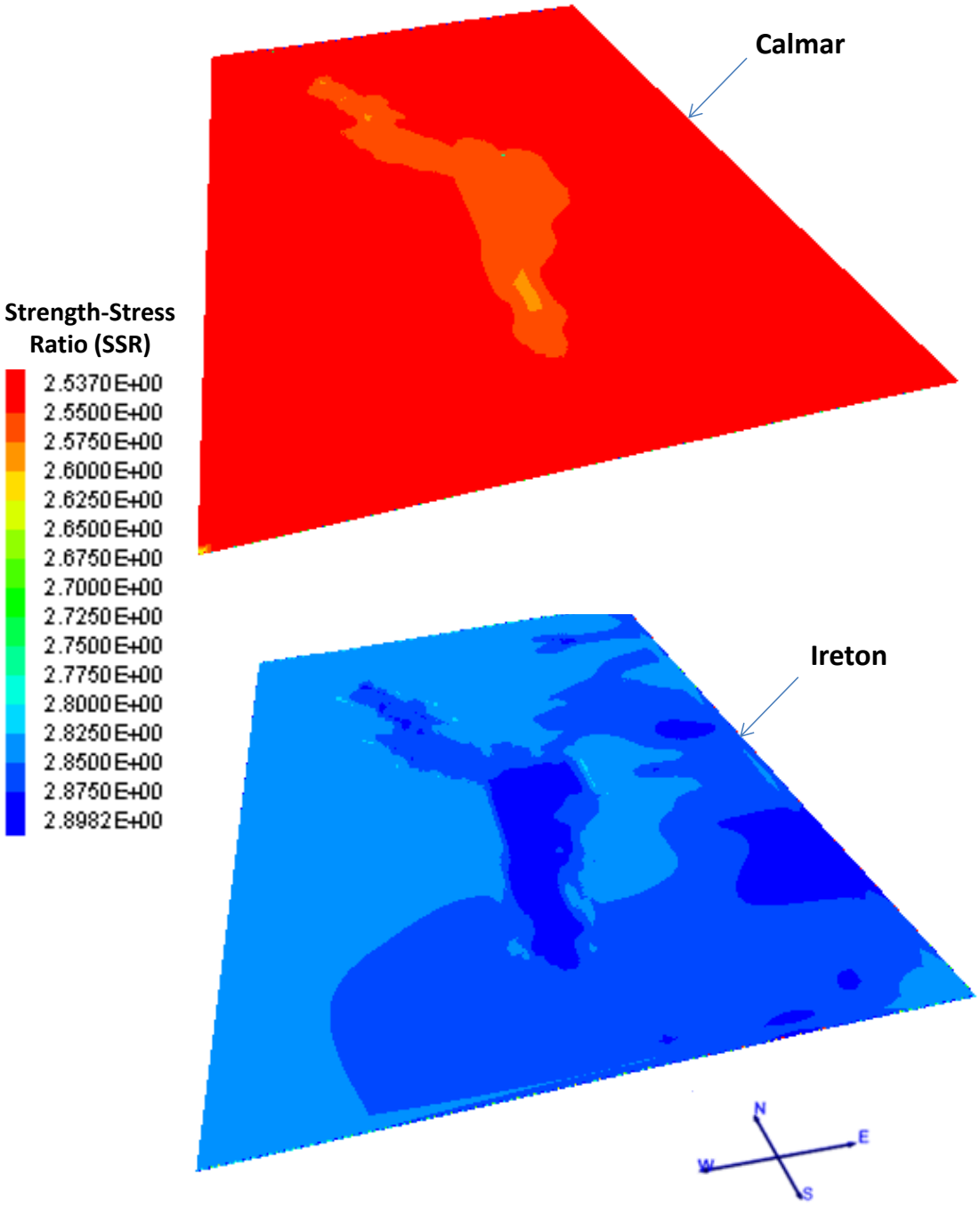

Figure D.4: Distribution of strength-stress ratio for fault reactivation ($SSR_{reactivation}$) for the Ireton and Calmar units after CO_2 injection.